

Spatial Signatures

Understanding (urban) spaces through form and function

July 2021

ABSTRACT: This paper presents the notion of spatial signatures as a characterisation of space based on form and function designed to understand urban environments. How we spatially arrange the building blocks that make up a city matters. On the one hand, it encodes many aspects of the phenomena that created such an arrangement in the first place. On the other, once in place, this arrangement of urban form and function underpins many outcomes, from economic productivity to environmental sustainability. Our approach unfolds in three main stages. First, we propose a new spatial unit –the Enclosed Tessellation (ET) cell– to delineate space in a way that is exhaustive and matches the underlying processes at which urban form and function operate. Second, we propose to attach a large variety of form and function-based characters to ET cells to describe each of these units. Third, to build spatial signatures, information on ET cells can be clustered using unsupervised learning techniques. This process results in a theory-informed, data-driven typology of space that follows form and function. We illustrate this approach by applying it to a sample of five very different cities scattered across the world. Our results demonstrate the ability to successfully differentiate different parts of a city that were built at different points in time and under different technological regimes, but also highlight broader comparisons about the nature of urban fabric in different regions. Our contribution resides in leveraging modern data, technology and methods to propose a detailed, consistent and scalable methodology that characterises urban form and function. The spatial signatures can be used across academic disciplines and by a variety of practitioners and policymakers supporting initiatives such as the Sustainable Development Goals.

Key words: Geographic Data Science, Urban Form, Urban Function

1. Introduction

How we spatially arrange the building blocks that make up a city matters. The map of many European cities tells the story of the different historical periods in which they were born, grew and, in some cases, contracted. American cities which “came of age” in the second half of the 20th Century would look very different had the automobile not been the defining technology of the time (Jacobs, 2016). And the stark contrasts between luxury developments and informal settlements that can be observed across many cities of the Global South are a reflection of the wide range of disparities and inequalities that those societies display (AlSayyad and Roy, 2003). This encoding of history, technology, and culture is sticky: once in place, elements of the urban fabric change slowly over time. Although cities are constantly in flux, new innovations and waves of change rarely start from scratch. More commonly, they are added in a layered way. Over time, each phase, each change blends in with the rest of the urban fabric to give a city its uniquely distinct pattern that defines it almost as a strand of DNA. The building blocks of this process include the different elements of the built and natural environments of which cities are composed, but also the purpose they serve. Understanding the former thus requires us to consider urban *form*, while grasping the latter invites us to examine its *function*. Urban form and function are relevant for two main reasons. First, their fabric encodes the socio-economic history, technology and values of the society that has built them. Studying the nature and distribution of form and function in cities thus helps us better understand the societies that, over time, have shaped them. Second, urban form and function are not only a history book recording the past, but also play an important role in defining the present and shaping the future. Once in place, their features and structure have direct implications for a wide range of outcomes, from productivity and job access to social inclusion and mobility, deprivation, service provision, energy consumption or carbon emissions, to name just a few. In this context, the main contribution of the present paper is to introduce the concept of spatial signatures as a characterisation of space based on form and function designed to understand urban environments. Our proposal contributes to the literature by filling a series of

existing gaps, including conceptual fragmentation and lack of detailed evidence at scale.

The study of urban form and function is deeply fragmented (Kropf, 2014, Brenner and Schmid, 2015, Gauthier and Gilliland, 2006). Work with this focus is scattered across different academic disciplines and policy-making scenes. This is not necessarily a problem in itself since different backgrounds provide a richer picture. And there is much to be gained from a plurality of perspectives. It does however mean that the evidence available presents different interests as well as varying degrees of detail, consistency, and coverage. It is understandable that economists develop conceptualisations shaped around economic theories (eg. Ahlfeldt and Pietrostefani, 2019), while geographers do so paying attention to spatial scales (eg. Boeing, 2018), and yet other disciplines bring different aspects to focus. Similarly, decision-makers interested in understanding aspects of urban form and function tend to see it through the lenses provided by the vantage point they occupy. Regional planners may try to obtain as much detail as possible for a relatively small geographical area (eg. Adjuntament de Barcelona, 2018); while supra-national organisations may

prioritise scale and coverage at the expense of detail (eg. EEA, 2016).

There is a clear need for detailed, consistent, and scalable evidence on urban form and function. Granular measurement that can be performed across large geographical extents in a comparable way can unlock insights that get lost when we only consider their parts in isolation. Similarly, analysis at scale that lack sufficient detail also miss important aspects. This is because many of the theoretical underpinnings of urban form and function that reflect its history and influence present and future outcomes tend to operate at fine scales; but, to be able to observe meaningful differences, we need to consider many and different places. For example, the characters that define Medieval city centres in Europe quickly blur when the geographical unit considered is coarse. But, to be able to examine how these characters relate to different levels of walkability, or even of gas emissions, we require a large extent to set up meaningful comparisons.

Of detail, consistency and scale, the current research landscape described above is able to provide, at best, any combination of pairs from those three (Jochem et al., 2020, Araldi and Fusco, 2019, Fleischmann et al., 2021b). There is an abundance of detailed studies that measure form and function in an internally consistent way, but these are in their majority confined to case studies with very limited geographical extents. On the other end of the scale spectrum, recent years have seen the appearance of work at a global scale that is internally consistent. However, their degree of detail tends to be hindered by data limitations. Finally, one could understand the multitude of detailed case studies in conjunction as a growing body of evidence that is able to reach a sizeable scale. But, in these case, the fragmentation discussed earlier often translates in a lack of consistency that prevents meaningful comparisons.

Recent advances in data, technology, and methodology are beginning to overcome these limitations. New forms of data such as open cadastres, consumer datasets derived from modern business operations, or high resolution, public satellite imagery are greatly improving the descriptions we can build of cities (Arribas-Bel, 2014, Glaeser et al., 2018, Wei et al., 2020, Fleischmann et al., 2021a). Progressively, we are able to build denser and more up to date representations of urban environments at a cheaper cost. Technological developments such as the dramatic increase of computational power available to researchers, or improvements in computer algorithms and machine learning are lowering the entry barrier to advances that only a few years ago required a high degree of dedicated expertise to be able to benefit from. Perhaps more importantly, recent methodological contributions such as morphometrics (Dibble, 2016) or geographic data science (Singleton and Arribas-Bel, 2021) are paving the way to blend these advances with domain knowledge and urban theory, effectively enabling disciplines concerned with the form and function of cities to benefit from such developments.

The spatial signatures are thus a delineation that divides geographical space based on its appearance (form) and how it is used (function). It is not a classification of space as much as a way of thinking around classifying space based on form and function. The concept is data-driven but theoretically informed; granular but scalable; and flexible enough to be adapted to a wide variety of applied contexts, from data-rich to those with limited availability. Spatial signatures embed theoretical ideas about how cities are spatially arranged, how this configuration can be best conceptualised, and how it is perceived by humans into a data-driven framework that

connects them to the vast amount of empirical information available representing the world. These theoretical underpinnings are sourced from a variety of disciplines, from architecture to environmental sciences, and thus are inherently interdisciplinary. The spatial signatures thus provide a shared vocabulary to bring together a variety of scholars and policy makers for whom form and function in cities is relevant, either as their main object of study or as an input for their own domains of expertise. These characteristics make the spatial signatures an ideal candidate for deployment on a wide range of data landscapes and geographical regions. To demonstrate this flexibility, Section 4 presents five illustrations that each apply the concept of spatial signatures to a different city, developing internally consistent classifications for each of them. It is important to emphasize we view these illustrations as a way to empirically showcase our conceptual proposal rather than as the empirical, main contribution of the paper.

In part because of their adaptability, the spatial signatures hold important potential both for urban academics and policy-makers. From an academic point of view, they are relevant as a goal in themselves that allows us to better measure and study the spatial configuration of the building blocks that make up cities. But they also represent a platform on which other disciplines can build on to embed form and function on a variety of socio-environmental outcomes. For policy-makers, the spatial signatures provide a framework for detailed spatial understanding of the cities and territories their decisions affect. They are useful both in the global north, where cities are constantly recast and retrofitted, as well as the global south, where most of the new urbanisation is currently taking place. In summary, the spatial signatures allow us to move forward in realising detailed, consistent, and scalable measurement of form and function in cities.

The remaining of the paper is structured as follows. Section 2 reviews existing literature on urban form and function, highlighting current gaps. Section 3 represents the core of our contribution by detailing our proposal of spatial signatures, including how we define them, the spatial unit we develop to measure them –the enclosed tessellation cell–, and the embedding of form and function into such unit. In Section 4, we illustrate the flexibility of the spatial signatures by presenting five illustrations of the spatial signatures to rather different global cities. And we conclude in Section 5 with some reflection about the value and potential of our approach.

2. (Urban) form and function

2.1 Form

Urban form approaches environments from the perspective of their physical structure and appearance. Research studying urban form has a long tradition, dating back to the early 1900s (Geddes, 1915, Trewartha, 1934). Urban morphology, subsequently, begun in the 1960s as an independent area of research. The field originated in parallel within geography (Conzen, 1960) and architecture (Muratori, 1959), reflecting its inherently multi-disciplinary nature, later reinforced by the inclusion of socio-economic elements, as in the work of Panerai et al. (1997). The original methods are predominantly qualitative, a tendency that persists today (Dibble, 2016). The first notable quantitative approaches date to the late 1980s and 1990s, reflecting advancements in computation and newly available data capturing the built environment. In this context, two strains of research

have emerged. One focuses on cartographic (vector) representation of the urban environment, assessing its boundaries (Batty and Longley, 1987), street networks (Hillier, 1996, Porta et al., 2006) and other elements (Pivo, 1993). The second one is based on earth observation, exploiting remotely sensed data to capture change in the footprint of urban areas (Howarth and Boasson, 1983).

The current state of the art still retains this distinction between cartographic and remotely sensed approaches. A modern quantitative branch of urban morphology, or urban morphometrics, has emerged working predominantly discrete elements of urban form, and proposing an abundant selection of measurable characters that describe different aspects of form (Fleischmann et al., 2020b). As part of this trend, methods focusing on a single aspect (Porta et al., 2006) have been replaced by efforts to better reflect the complexity of urban form through the combination of multiple morphometric characters into a single model, often leading to data-driven typologies (Song and Knaap, 2007). This focus on classification is becoming more prominent, fueled by the possibilities afforded by new datasets increasingly available. Indeed, the literature is now able to produce typologies that start from small-scale studies focused on blocks and streets (Gil et al., 2012), and zoom out into larger areas with higher granularity (Schirmer and Axhausen, 2015, Araldi and Fusco, 2019, Bobkova et al., 2019, Dibble et al., 2019, Jochem et al., 2020).

Advances in remote sensing have also led to a range of classification frameworks based on various conceptualizations of the urban fabric. However, there is one significant difference between classification derived via morphometric characterization and the one based on remote sensing. Where the former is mostly unsupervised (Araldi and Fusco, 2019, Schirmer and Axhausen, 2015), exploiting the hidden structure in the data to develop organically the typology; the latter tends towards supervised techniques, relying on classes defined a priori (Pauleit and Duhme, 2000). Two emerging classification models used to inform these exercises are Local Climate Zones (Stewart and Oke, 2012), defining ten built-form types and seven land cover types, and used recently by Koc et al. (2017) or Taubenböck et al. (2020); and the Urban Structural Type, a generic typology based on the notion of internal homogeneity of types (Lehner and Blaschke, 2019).

2.2 Function

Urban function considers environments based on the activities that take place within them. The focus is thus not on what a space “looks like”, as it is the case on urban form, but on “what it is used for”. What activities occur within cities, how they are spatially configured, and how they relate to each other are key questions in this context. To the extent cities compress space and time to concentrate human activity of very diverse nature, the study of function is relevant to a variety of fields and is undertaken by a wider constituency of researchers. Disciplines as disparate as geography, economics or environmental sciences have contributed in their own way to our understanding of urban function. Furthermore, because function has direct implications for a wide range of social and environmental processes at different geographic scales, their study also falls within the realm of policy. Given the breadth of perspectives and goals, a complete overview of its contributions is beyond the scope of this paper. Instead, here we highlight what we consider

the most relevant domains involved: environmental sciences, urban and public economics, urban and transport geography, planning, and sociology.

Environmental sciences have long considered urban function in the context of the broader interest on understanding the natural characteristics of the surface of the Earth. An area that has attracted much effort relates to the development of classifications of land cover and land use, the former describing the nature of surfaces while the latter focusing on how those surfaces are used. Several land cover classifications are available (e.g. CORINE, European Environment Agency, 1990, in Europe; the National Land Cover Database, Homer et al., 2012, in the US; or the Land Cover CCI, Defourny et al., 2012, globally), as well as some for land use (e.g. the Urban Atlas project, Copernicus Land Monitoring Service, 2021). While much of this research is not focused on urban environments, the urban remote sensing community (Weng and Quattrochi, 2018) is building a more explicit bridge between these approaches and the study of cities (e.g. Kuffer et al., 2016, Georganos et al., 2018, Jochem et al., 2018, Prasad, 2015, Stark et al., 2020). Note that, within this work, “urban function” is not equal to land use but is seen as a broader term. In practice, land use is considered to be only one aspect of function.

A wide array of disciplines have developed more specific interests in urban function. Sustainability studies, for example, are interested in how function is configured within and across cities in so far as it relates to the level of emissions (Angel et al., 2018) or energy consumption (Silva et al., 2017). The social sciences have a long-standing interest on the spatial configuration of form because it affects several outcomes of prime interest. Depending on the nature of these outcomes, form is conceptualised in one or another way. Urban economics pays special attention to density of economic activity and, by extension, of population (Ahlfeldt and Pietrostefani, 2019, Duranton and Puga, 2020), since density is intimately related to theories of agglomeration, one of the intellectual pillars of the field. Public economics has paid attention the configuration of urban function to the extent that it determines the efficiency of certain public services provided by local governments (Carruthers and Ulfarsson, 2003, Hortas-Rico and Solé-Ollé, 2010). Sociologists and planners have also found that different spatial configurations of function over space is associated with different degrees of social mobility (Ewing et al., 2016) or socio-economic deprivation (Venerandi et al., 2018). More generally, transport researchers have built a robust body of knowledge linking urban function and its spatial distribution to travel behaviour (Boarnet et al., 2001), sustainability (Sevtuk and Amindarbari, 2020), or accessibility to jobs (Horner, 2004) and amenities (Diamond and Tolley, 2013), with clear implications for socio-economic disparities.

2.3 Blending Form & Function

Whilst much of the literature focuses either on form or function, the two are deeply interconnected. Function develops in the context provided by form; and, over time, form adapts and encodes function. However, there exists a few attempts to classify urban spaces considering both jointly. Bourdic et al. (2012) propose a comprehensive classification based on indicators ranging from form to biodiversity, culture and energy on a scale of individual cities. Several studies consider the link between form and land use (Song and Knaap, 2007, Song et al., 2013, Bourdic et al., 2012), with some authors even including land use a component of form characterisations (Dibble et al.,

2019). At any rate, even when the two are combined, the scope of either, particularly function, is narrow rather than all-encompassing. For example, the geodemographic tradition (Harris et al., 2005, Webber and Burrows, 2018) studies populations based on where they live. Although this considers both, the focus is very much on the residential function, leaving aside others such as employment or amenities. Recent years have also seen work at the global scale connecting form and population density (Ewing et al., 2002, Zheng et al., 2014, OECD, 2018), many facilitated by the appearance of new datasets (e.g. Pesaresi et al., 2019, Sorichetta et al., 2015), alongside studies embedding accessibility and proximity to points of interests into their frameworks (Alexiou et al., 2016, Venerandi et al., 2019). Nevertheless, the body of research directly working with both form and function in a single framework is limited and tends to focus on particular functions.

3. Spatial Signatures

Despite the current sparsity of studies, we believe there are several benefits in considering form and function in tandem when trying to understand urban spaces. The two are deeply interconnected. This close correlation implies that outcomes observed across form tend to hold true for function, and viceversa. However, unique patterns emerge when particular types of form and function come together. We argue that it is only through the combination of form and function that cities are able to encode and reflect sophisticated aspects of human nature such as history, culture or technology. In these cases, considering only one or the other hinders rather than enables, as we risk missing important traits of the nature of a place. From a more empirical perspective, even when the two dimensions mostly overlap, there is value in considering them jointly. Some aspects of form and function, like human perception of space, are influenced by both and, while clear conceptually, they can be challenging to measure. Broadening the pool of indices that can be deployed ensures better accuracy when characterising existing patterns on the ground. In this section, we detail our proposal to understand urban form and function through what we term “spatial signatures”.

3.1 Definition

We propose the notion of *spatial signatures* as:

A characterisation of space based on form and function designed to understand urban environments

Spatial signatures provide exhaustive coverage for an area of interest by drawing organic boundaries that delineate portions of consistent morphological and functional characteristics. We will refer to a single *spatial signature* in two related but distinct ways: first, as one of the multiple classes that make up a wider typology of spatial signatures; and second, as a geographical instance of that class, a contiguous portion of territory that shares those morphological and functional traits. As such, spatial signatures can be seen as organically grown delineations that organise space into urban and rural, orderly and irregular, formal and informal. Laid out together, they can be used to explore urban extents, to parse through the complexity of their spatial structure, or to understand the evolution of cities. In bringing together both form and function,

with a focus on the urban, spatial signatures provide a nexus between purely morphological characterisations and those entirely based on function. To the extent form and function are intrinsically connected, its combination leads to more robust portraits of the space that makes up cities. And, since the focus is on the urban, spatial signatures provide a complementary perspective to most land cover and use classifications, which historically pay more attention to the portion of space not occupied by cities. Developing the concept of spatial signatures rests on two key pillars: the spatial unit of choice and the embedding of urban form and function into such units to be able to delineate signatures. We turn to both of these in more detail now.

3.2 Building blocks: the Enclosed Tessellation

This section proposes a novel and theoretically-informed delineation of space to support the development of spatial signatures. Since spatial signatures are conceptualised as highly granular in space, considering the ideal unit of analysis at which to measure them is of utmost importance. This step is worth spending energy and effort for two main reasons. First, if ignored, there is an important risk of incurring the modifiable areal unit problem (MAUP, Openshaw, 1981). The urban fabric is not a spatially smooth phenomenon; rather, it is lumpy, irregular and operates at very small scales. Choosing a spatial unit that does not closely match its distribution will subsume interesting variation and will hide features that are at the very heart of what we are trying to capture with spatial signatures. Second, and conversely, we see adopting a meaningful unit a step of analysis itself. Rather than selecting an imperfect but existing unit to try to characterise spatial signatures, delineating our own is an opportunity in itself to learn about the nature of urban tissue and better understand issues about distribution and composition within urban areas.

Let us first focus on what is required from an ideal unit of analysis for spatial signatures. We need a partition of space into sections of built *and* lived environment that can later be pieced together based on their characteristics. The result will feed into an organic delineation that captures variation in the appearance and character of urban fabric as it unfolds over space. To be more specific, a successful candidate for this task will need to fulfill at least three features: indivisibility, internal consistency, and exhaustivity. An ideal unit will need to be *indivisible* in the sense that if it were to be broken into smaller components, none of them would be enough to capture the notion of spatial signature. Similarly, every unit needs to be *internally consistent*: one and only one type of signature should be represented in each observation. Finally, the resulting delineation needs to be geographically *exhaustive*. In other words, it should assign every location within the area of interest (e.g. a region or a country) to one and only one class.

The existing literature does not appear to have a satisfying candidate to act as the building block of spatial signatures. Without attempting an exhaustive review, an endeavour beyond the scope of this article, the vast majority of existing approaches to delineate meaningful units of urban form and function fall within one of the following three categories. The first group relies on *administrative* units such as postcodes, census geographies or municipal boundaries (e.g. Taubenböck et al., 2020). These are practical as they usually are readily available. However, their partition of space is usually driven by different needs that rarely align with the measurement of spatial signatures, or indeed those of any morphological or functional urban process. Taubenböck

et al. (2019) even argue that “administrative units obscure morphologic reality”. An emerging body of work relies on granular, *uniform grids* as the main unit of analysis (e.g. Jochem et al., 2020). This choice is usually explicitly or implicitly motivated by the lack of a better, bespoke partitioning; the use of input data distributed in grids (e.g. satellite imagery); and the assumption that, with enough resolution, grids can be organically aggregated into units that match the processes of interest. A third approach followed mostly by the literature on urban morphology relies on the definition of morphometric units. These include street segments (Araldi and Fusco, 2019), plots (Bobkova et al., 2019), building footprints (Schirmer and Axhausen, 2015), or constructs such as the Sanctuary area (Mehaffy et al., 2010, Dibble et al., 2019). In all these cases, the choice is justified by the particular application in which it takes place. However none of these approaches meet the three characteristics we require for spatial signatures. Administrative boundaries are exhaustive but rarely indivisible or consistent when it comes to urban form, usually grouping very different types of fabric within a single area. Uniform grids are also exhaustive but the arbitrariness of their delineation with respect to urban form leaves them divisible and internally inconsistent. Even high resolution grids (i.e., very granular cells) might not be an ideal approach to capture the variability of urban form and function over space.¹ Morphometric units are the most theoretically appealing ones since they are built to match the distribution of urban features and are usually granular enough to warrant internal consistency and indivisibility. Most of them are however not exhaustive as they are anchored to particular elements of the built environment, such as streets or building footprints, which do not provide full coverage. Plots would theoretically meet all characteristics but can be problematic due to their variable definition leading to different geometric representations (Kropf, 2018).

We propose the development of a new spatial unit that we term the *enclosed tessellation cell* (EC). An EC is defined as:

The portion of space that results from growing a morphological tessellation within an enclosure delineated by a series of natural or built barriers identified from the literature on urban form, function and perception.

Let us unpack this concept a bit further. ET cells result from the combination of three sequential steps (Figure 1). First, they rely on a set of enclosing components: features of the landscape that divide it in smaller, fully delimited portions. The list of what should be counted as enclosing is informed by theory and, as we will see below, may vary by context. But, as an illustration, it includes elements such as the street network, rivers and coastlines, or railways. Second, these enclosing features are integrated into a single set of boundaries that partition the geography into smaller areas. In some cases, they will be small, as with urban blocks in dense city centres; in others, they will be larger in size, as in rural sections with lower density of enclosing features. We call each of this fully delimited areas an enclosure. Third, enclosures are further subdivided using a morphological tessellation (Fleischmann et al., 2020a), a method derived from Voronoi

¹For example, areas with little variation in form and function, such as large parks or natural spaces, would be overrepresented in that it would take many cells to cover a single morpho-functional unit. At the same time, a single cell in areas with more intense variation of form and function, such as city centres, would aggregate more than one unit into a single cell. At the heart of this behaviour is the fact that uniform grids account for space in a directly proportional way to their area. This is not how form and function unfolds spatially.

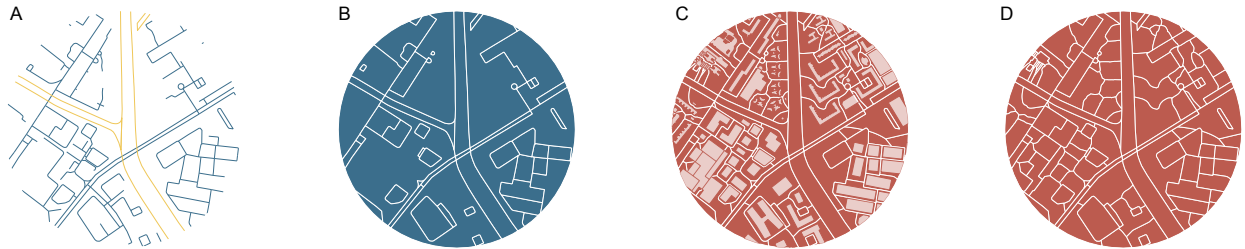


Figure 1: Diagram illustrating the sequential steps leading to the delineation of enclosed tessellation. From a series of enclosing components, where blue are streets and yellow river banks (A), to enclosures (shown as blue polygons) (B), incorporation of buildings as anchors (C) to final tessellation cells shown as individual red polygons (D). Note that the resulting tessellation covers entirety of space, including the enclosures with no buildings on them (as the river in this case).

tessellation taking polygons instead of points as an input, that exhaustively partitions space based on a set of building footprints, which are used in this context as anchors to draw catchment polygons. This three-step process generates geographical boundaries for a given area that result in a new spatial unit. This unit provides full geographical coverage without any overlap. Since the essence of the approach resides in growing a tessellation inside a set of enclosing features, we call the resulting areas “enclosed tessellation cells”.

The enclosed tessellation (ET) intersects two perspectives of how space can be understood and organised. The first relies on the use of features that *delimit* the landscape and partition it into smaller, fully enclosed portions. These include the road and street networks, but also others such as railways or rivers. Each feature is conceptualised as a line that acts as a boundary, dividing space into what falls within each of its sides. A long tradition in the literature on urban perception relies on variations of these delimiters. Prominent early examples include the edges and paths highlighted by Lynch (1960) as two of the five core elements that define legibility and imageability of a city; as well as the later work inspired by this framework (e.g. Filomena et al., 2019).

The second perspective that ET integrate is a vision organised around *anchors*. In this view, space arises in-between a discrete set of relevant features. Unlike delimiters, these elements do not partition space per se, but instead act as origins to which the rest can be “attached”. The choice of anchors might vary by context but, in this case, the literature on morphometrics has extensive evidence to support the use of buildings as the primary feature (Hamaina et al., 2012, Usui and Asami, 2013, Schirmer and Axhausen, 2015).

The combination of delimiters and anchors as the parsers of space make ET cells an ideal spatial unit to study spatial signatures, one which meets the three requirements we outlined above. They are indivisible in that a single EC will contain no delimiters, at most a single anchor, and potentially none. They are also internally consistent because they are delineated as the area within the delimiters that contain at most one anchor. And finally ET cells are exhaustive in that every location within the area of interest is assigned to one and only one EC, providing full geographical coverage without any overlap. Due to space and focus constraints, we do not compare them empirically to competing alternatives such as administrative units or uniform grids, but we consider this endeavour a fruitful avenue for future research.

3.3 Embedding form and function into spatial signatures

This section covers the development of spatial signatures from a set of ET cells. ET cells take the role of the structural unit. In themselves, they hold descriptive value in reflecting the configuration of the urban environment. They also operate as a container, into which other morphometric and functional characters can be embedded. To "fill" these containers with more information, we propose to collect a set of descriptors reflecting both form and function so that, together, they capture an intertwined representation of both dimensions. In practice, this process will lead to a heterogeneous mix of morphometric characters, capturing patterns of physical, built-up environment; and functional characters, reflecting economic activity, amenities, land use classification or historical importance.

Table 1: Excerpt of form characters used in the Barcelona case study. Implementation details are provided in Jupyter notebooks available at <anonymised for peer-review>. The categorisation follows Fleischmann et al. (2020b).

index	element	context	category
...
area	building	building	dimension
perimeter	building	building	dimension
circular compactness	building	building	shape
squareness	building	building	shape
solar orientation	building	building	distribution
street alignment	building	building	distribution
coverage area ratio	tessellation cell	tessellation cell	intensity
openness	street profile	street segment	distribution
degree	street node	neighbouring nodes	distribution
shared walls ratio	adjacent buildings	adjacent buildings	distribution
area	enclosure	enclosure	dimension
local meshedness	street network	nodes 5 steps	connectivity
local closeness centrality	street network	nodes 5 steps	connectivity
perimeter wall length	adjacent buildings	joined buildings	dimension
...

Which exact characters to compile for a particular implementation of spatial signatures will depend on the availability of data in that context. Since this section outlines the process conceptually, we do not consider including any specific list as useful as providing broad guidance on the kind of characters that should be aimed for when designing an application of the spatial signatures. Any selection in this respect should aspire to reflect the nature of form and function in the area of interest in as exhaustive a way as possible. As an example, Table 1 (2) contains an excerpt of Table 3 (4) in the supplementary material, which captures all of the form (function) characters we use in the Barcelona illustration of Section 4. We recommend building on the principles explored by Dibble et al. (2019) and Fleischmann et al. (2021b), and following the rules originally proposed by Sneath et al. (1973). These can be broadly summarised as *include as many characters present in literature as is feasible, while minimising potential collinearity and limiting redundancy of information*. This guidance includes all categories of form characters identified by Fleischmann

et al. (2020b) (ie. dimension, shape, spatial distribution, intensity, connectivity, diversity) and as wide as possible of a range for functional characters available for a given case study, including land cover/use, employment/economic activity, and amenities. While the optimal ratio of form to function characters is to be aimed at balance, this may not always be possible. Form characters can be derived from a small set of data sources (eg. street networks and building footprints) while describing function relies on a larger set of data. We do not see this as a limitation of the spatial signatures as much as one of data availability. If anything, the joint approach of form and function encouraged by our proposal ameliorates the problem given the interrelations between form and function described above and that function has been found to be implicitly present in the description of form (Caniggia and Maffei, 2001 in Kropf, 2009).

The above implies that classifications based on different sets of data will inevitably be different, even if applied to the same geographical region. Such property is not unique to spatial signatures. In fact, most widely used classification approaches in urban studies (e.g., land-use classifications, geodemographic classifications) share it. More than a limitation, we see this as evidence of their flexibility: signatures provide a framework to quantify form and function which can adapt to the characteristics, availability, and quality of the data available.

Table 2: Excerpt of function characters and transfer methods used in the Barcelona case study. Implementation details are provided in Jupyter notebooks available at <anonymised for peer-review>.

character	input spatial unit	transfer method
...
population	block	Building-based Dasymetric mapping
number of other items that are not premises	block	Dasymetric mapping
land use	parcel	Spatial join (centroid)
number of dwellings	building	Attribute join
parks	points	Accessibility - distance to nearest / # within 15min
restaurants	point	Accessibility - distance to nearest / # within 15min
trees	points	Spatial join (count)
NDVI	raster 1m	Zonal stats
...

Since spatial signatures are capturing contiguous spatial patterns, characters need to be able to encode it. Therefore, instead of treating values measured on each ET cell independently, we also propose to incorporate features from the immediate spatial *context*. Our preferred definition of context relies on ten topological steps from every ET cell as illustrated on figure 2). Each of the ET cells within this limit is then weighted according to its metric distance from the original cell, ensuring that the cells that are closer are influencing the result more than those that are furhter

away. The resulting weighted distribution of values is then used to sample three proxy variables - the first, the second and the third quartile, capturing the tendency of individual values in the area.

Collecting characters at the ET cell level is only half the task to develop spatial signatures. Given the granularity and multi-dimensionality of the information at this stage, we need to combine it in a way that retains its core characteristics but is easier to parse through. We propose a feasible aggregation of ET cells into spatial signatures using unsupervised learning. Again, it is not the role of this section to single out a technique, since many exist including K-Means, gaussian mixture models, or self-organizing maps (Kohonen, 1990), to name a few. We note there is no need to impose a spatial contiguity constraint as spatially contiguous clusters of cells in the same signature will emerge thanks to the inherent spatial autocorrelation of data derived from mutually overlapping *contexts*. These continuous groups of cells grouped in the same cluster is what we call instances of a spatial signature.

4. Illustrations

In this section, we present five different illustrations of how the concept of the spatial signatures can be applied in a variety of scenarios, including a set of diverse backgrounds and data landscapes. We propose the spatial signatures as a way to understand urban form and function, and they represent a conceptual framework that can be applied at scale while retaining detail. As such, any one application of this notion will materialise differently depending on the region of interest, details of the particular implementation (eg. clustering algorithm), and the nature of the data available. Though not directly comparable (eg. the classes delineated may differ depending on unique regional characteristics), we view the development of spatial signature classifications for different regions as valuable. Indeed, the exploration of how to bring different classifications into dialogue to meaningfully extract similarities and differences of the urban systems they represent is a fruitful avenue of research. This section thus *illustrates* how the concept of spatial signatures can be operationalised in a variety of contexts. In doing so, we demonstrate the flexibility of our conceptual proposal to adapt to a variety of inputs and case-by-case idiosyncrasies, while retaining the merit of the concept. In this respect, each of the illustrations can be seen as an instance of developing granular and (internally) consistent classifications that can be deployed at scale.

We intentionally select a set of diverse locations. The five cities chosen are displayed in Figure 3. The sample offers geographical variation covering Europe (Barcelona, Spain), North America (Houston, TX, United States), South America (Medellin, Colombia), Africa (Dar es Salaam, Tanzania) and South-east Asia (Singapore). Additionally, each city embodies different cultural backgrounds, planning paradigms involved in shaping the respective environments, as well as varied historical and social contexts in which the selected cities were built and developed. From a technical point of view, the selection brings a variety of input data covering both extremes in terms of quality (e.g., official mapping in Barcelona vs remote sensing-derived in Houston), the richness of information on functional aspects of places (e.g., detailed data on the municipal level

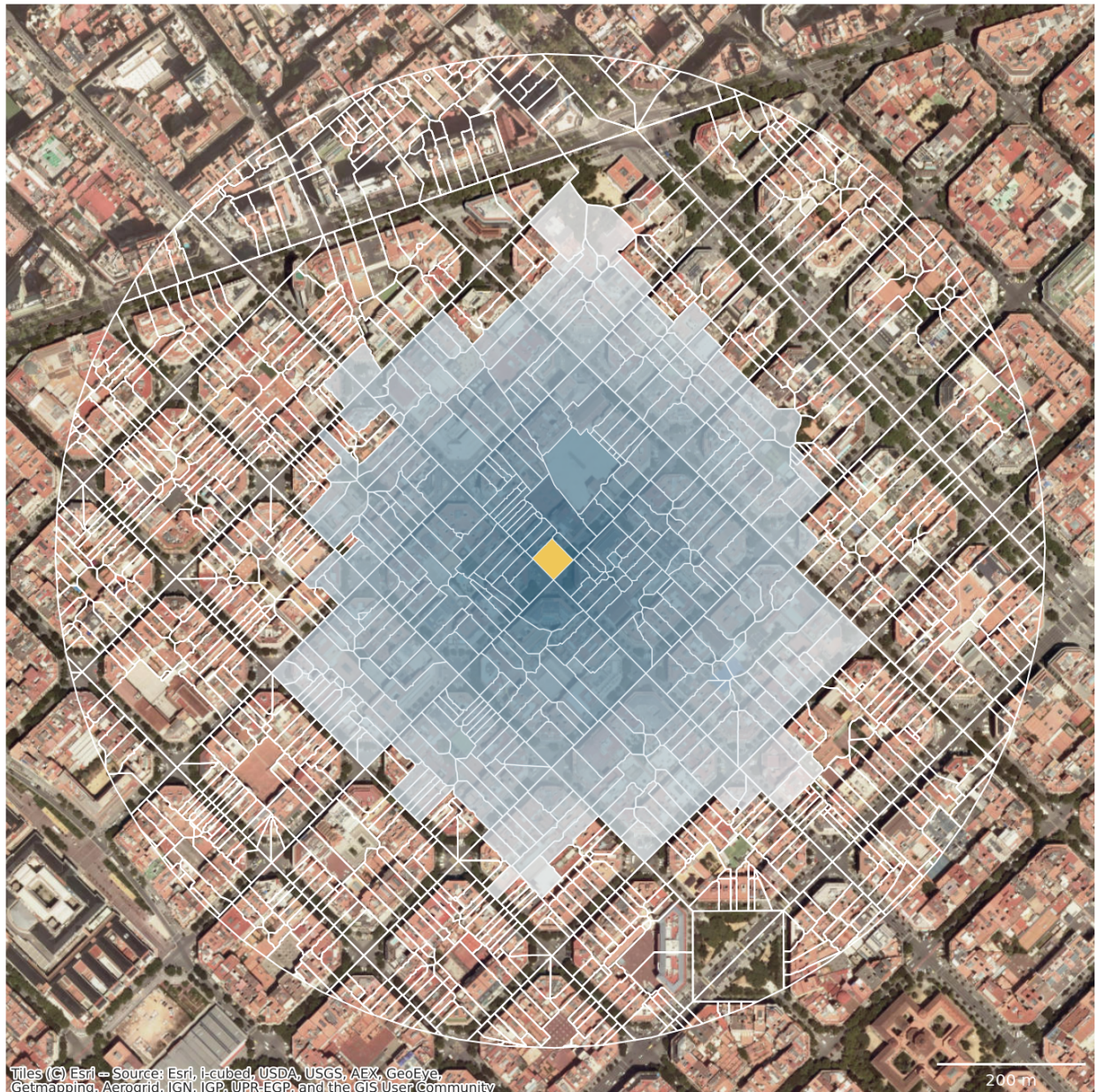


Figure 2: Illustration of a definition of spatial context used to capture the distribution of values around each ET cell. For the yellow ET cell in the middle, we propose to define a neighbourhood of 10 topological steps on the tessellation (each step represents a movement from one cell to a neighbouring one) and weigh the importance of each cell within such an area by inverse distance between cell centroids.



Figure 3: Selection of case studies covering geographical variation, cultural diversity, different planning paradigms involved in shaping the respective environments as well as varied historical and social contexts in which the selected cities were built.

in Medellin vs global gridded datasets in Dar es Salaam) and scale (82,375 units in Barcelona vs 2,043,581 units in Houston).

4.1 Method

The delineation of spatial signatures starts with the input data reflecting form and function of each place. We use enclosed tessellation, outlined in Section 3.2, as the core spatial unit. Therefore, the input data consists of building footprints and physical barriers –delimiters– denoting streets, railways, and water bodies. Using these delimiters, we first identify the geometry of enclosures, which we combine with building footprints to grow ET cells. The resulting set allows for a comprehensive morphometric analysis composed of characters capturing individual aspects of form, and contextualisation, following the model proposed by Fleischmann et al., 2021b. In the latter, we include the distribution of each character within the neighbouring context of each tessellation cell. Function is captured as a heterogeneous set of characteristics reflecting features from population density to location of amenities. All aspects are linked to ET cells using the most appropriate method for each data input (e.g., areal interpolation, network accessibility). The complete list of used characters reflecting both form and function, as well as implementation details are available in Appendix A.

It is to be noted that each case study uses a different set of characters, depending on the local data landscape. While that would be an issue if we wanted to directly compare signatures identified in all case studies within a single analysis, it is not an issue within this paper. We are including geographically varied cases to illustrate the versatility of the method and its applicability in different contexts rather than developing a single classification covering all five cities.

Spatial signatures are then identified using cluster analysis on the form-function characteristics attached to ET cells. The combined data reflecting both form and function are therefore standardised and clustered using K-Means. Since the number of classes is not known a priori, we use

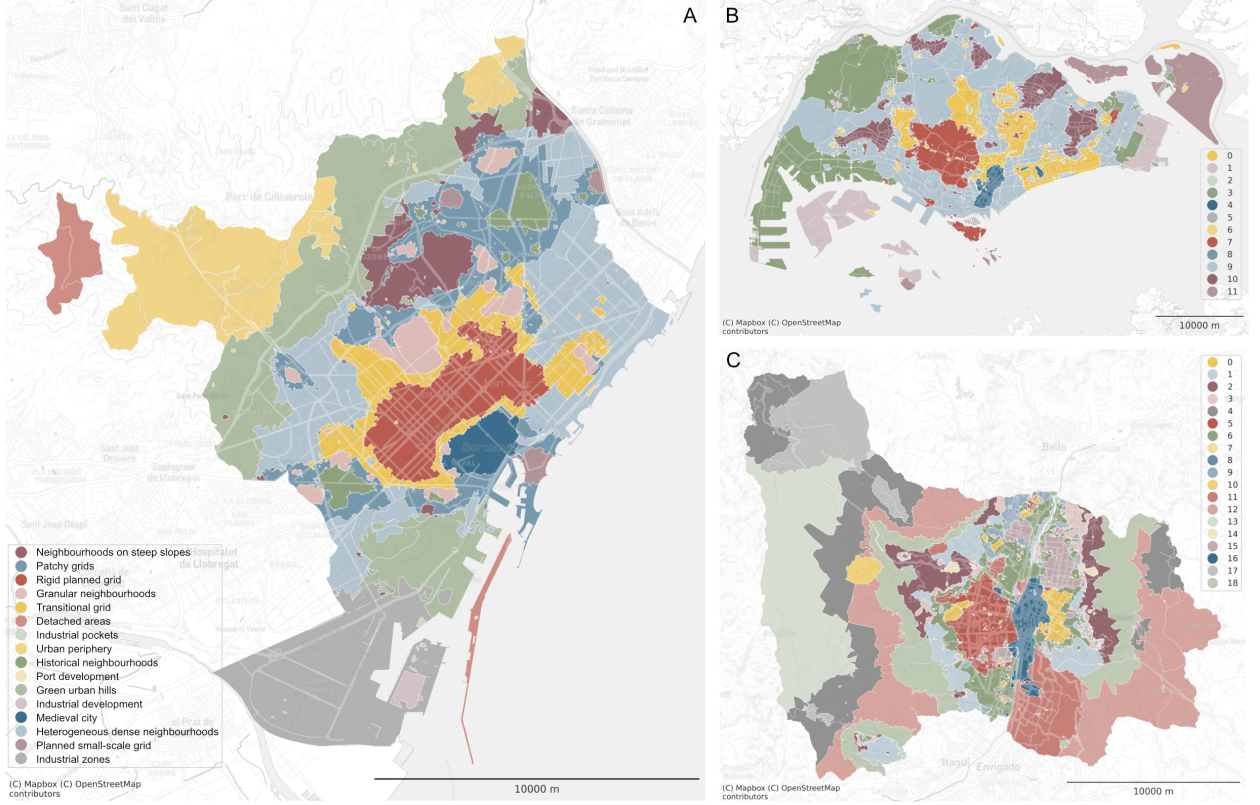


Figure 4: Resulting spatial signatures in the case of Barcelona (A), Singapore (B) and Medellin (C). Colours are used to distinguish between types within a single case, there is no relation of colours across the case studies. Barcelona case study illustrates possible interpretative naming of signatures. Note scale differs across maps given the different extent covered by each urban area.

clustergrams (Schonlau, 2002) to understand the behaviour of different solutions and select the optimal number of groups. The optimal number is then selected based on the stability of cluster branching. Appendix A contains details on the clustergrams used. The final clustering is run with 1000 initialisations to ensure stability of results. Once clustered, we aggregate contiguous ET cells assigned into the same cluster to create instances of spatial signatures.

4.2 Results

Figures 4-5 illustrate the resulting spatial signatures in the respective case studies. The geometries reflect the spatial extent of individual signatures derived from the enclosed tessellation with colour coding reflecting the type of a signature, i.e. the initial cluster. Two areas within the same type are expected to share form and function characteristics, being more similar to each other than to the other classes. Note that the similarity of different colours does not encode similarity of signatures. Figures 11-15 show the numerical profile of each class as a mean value of each character and figures 16-20 histograms of the cluster abundance.

The granularity of classification, that is the number of classes identified through the clustergram, ranges from nine (Houston) to 19 (Medellin) signature types. However, it is interesting that the actual number is not dependent on the size of each city but rather on the heterogeneity in

form and function of each place. This phenomenon is best illustrated on the comparison between Houston and Barcelona, the largest (2 million cells) and the smallest (80 thousand cells) case. Houston, archetype of North American, post WW-II sprawling urban fabric shows considerably smaller diversity of spatial patterns (nine spatial signature types) than Barcelona (16 types). The distribution of cluster sizes follows the same unequal pattern across all cases. The most extensive types contain between 15% and 28% of all observations, gradually decreasing towards a small number of outlier clusters containing less than one per cent of all observations within each sample. All illustrations include both extremes on the urbanisation continuum, with delineated central districts on the one hand and non-urban countryside signatures on the other. We interpret this transition as a gradual move from more urban signatures to less so. The only exception where this pattern is not as clear (but still present) is Singapore, whose geographical extent is limited to the main island and thus does not allow for full transition.

Barcelona is known for its extension grid (“Eixample”), which is captured as a unique signature we name *Rigid planned grid*. However, this development is historically an infill between the city’s medieval core and smaller preexisting peripheric settlements. Both core and periphery are reflected in the typology of signatures, which embody these historical origins. The spatial transition between historical organic fabric and the heavily planned Eixample is reflected as another signature (*Transitional grid*), stitching together different patterns into a coherent city. As shown on figure 11, both are defined by small areas of ET cells, higher number of courtyards or linearity of street segments. However, they differ in the proportion of heritage, accessibility to cultural venues and parks or solar orientation of buildings (*Transitional grid* is more variable in that sense).

The spatial distribution of signatures in Medellin tells the story of its intricate topography, even though the input data do not contain any explicit information on it. The city lies in a valley surrounded by steep slopes. While the central parts are found on the relatively flat terrain allowing paradigmatic planning and regularity of form and function, hillsides become more vernacular leading to a sharp urban edge where topography limits further development.

Signatures in Dar es Salaam reflect changes in the degree of formality in development, with formal areas (yellow) distributed across the central parts of the city, in the vicinity of the coastline. The transition between different degrees of formality is not always gradual as most informal parts of the city (light green and dark blue) appear as infills of the space not occupied by more planned neighbourhoods.

The character of spatial signatures in Houston follows two primary principles. One forms the spine of activity spreading from the city centre radially to the suburbs. The other fills the areas in-between the former, suggesting the decline of compact, walkable urban blocks into the convoluted, dendritic street network patterns of modern suburbs. The change in these predominantly residential signatures is gradual and reflects the waves of development the city has experienced during the post-war period.

A similar situation can be found in Singapore, where different types of signatures can be linked to the period when they were developed. Contrary to previous cases, this evolution and, consequently, spatial signatures followed a radial pattern. This process is not entirely contiguous,

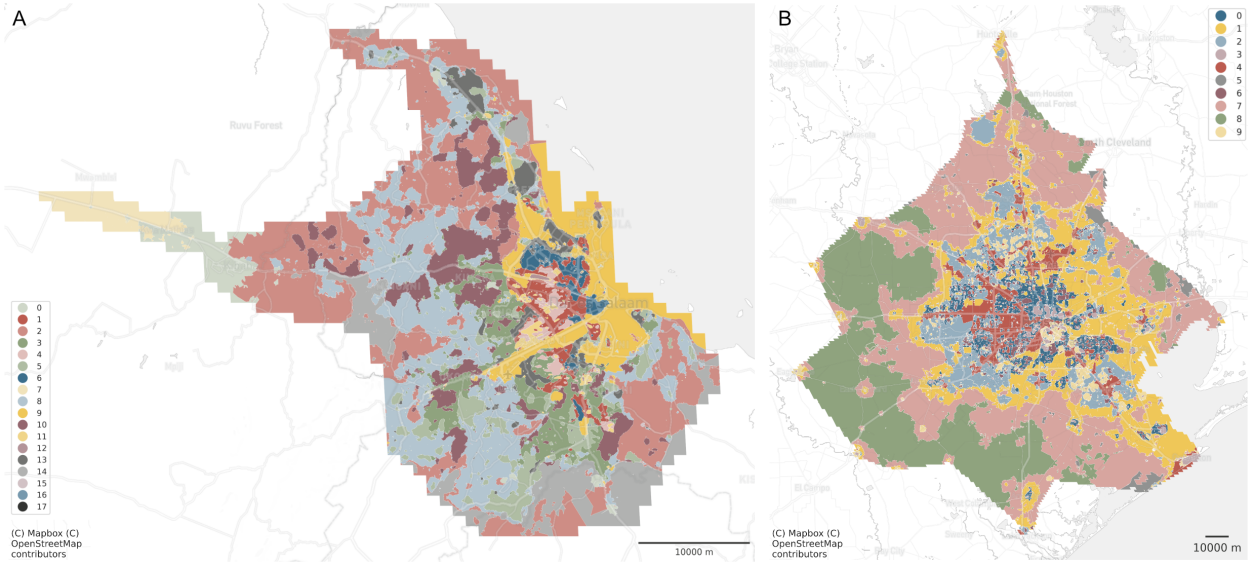


Figure 5: Resulting spatial signatures in the case of Dar es Salaam (A) and Houston (B). Colours are used to distinguish between types within a single case, there is no relation of colours across the case studies.

and thus appear major infills built in the last 50 years.

5. Conclusions

This paper proposes the notion of spatial signatures as a characterisation of form and function designed to understand urban spaces. As such, spatial signatures have the potential to provide unique insight into the ways human populations create and inhabit cities. Developing spatial signatures begins with a partition of space that is theoretically aligned with their purpose. To this end, we propose the enclosed tessellation. With appropriate spatial units at hand, we show how form and function can be quantitatively built in. Our contribution resides in the combination of a unifying approach to urban form and function with the proposal of a new spatial unit (the ET) that is theory-informed and data-driven. In this respect, spatial signatures bridge purely morphological approaches based on concepts like the morphological region (Oliveira and Yaygin, 2020), Local Climate Zone (Stewart and Oke, 2012) or Urban Structural Type (Lehner and Blaschke, 2019), with functional approaches such as land use/land cover classifications (Georganos et al., 2018) or mobility and population (Gale et al., 2016).

Rather than a particular technique or a rigid application, the spatial signatures provide a *way of thinking* about building detailed, scalable and internally consistent characterisations of form and function in cities. It is a way of conceptualising built (and natural) environment. The outputs from different regions or countries can be understood as different manifestations of similar concepts. Such dissimilarities in themselves can be indication of unique characteristics in the urban systems being compared. In this context, the spatial signatures can highlight and adapt to these circumstances, while retaining the intellectual consistency of a shared conceptual framework.

Differences in data availability between different regions of the world currently preclude planetary-scale analysis that are fully consistent and thus directly comparable. We do not see this as a limitation of the conceptual framework we propose in this paper but one of current data limitations. However, we believe this is a technical barrier that is constantly being lowered by technological (e.g., new forms of satellite-based data) and societal (e.g., user-generated databases such as OpenStreetMap) advances in data generation. As these new forms of global datasets become more and more sophisticated, the need for conceptual frameworks, such as the spatial signatures, that provide theory-informed ways of leveraging them will only increase.

The spatial signatures can be used by other researchers and policymakers interested in cities, their form, and how activity is distributed within them. While this article provides the conceptual underpinnings of our proposal, we also provide open-source software and documentation that can be freely used to generate ET cells from a variety of widely available datasets, and to attach form and function characters to those spatial units. We envision this approach, and its outputs from particular classifications, as a useful input to integrate urban form and function in research across disciplines such as geography, planning, economics or sociology. For example, because the spatial signatures synthesize many datasets into an intuitive, one-dimensional characterisation, they could be used in research that links the spatial structure of cities to their degree of sustainability, environmental performance, or economic productivity. Similarly, since they operationalise conceptual ideas about how our current cities can adapt to the main challenges of the century, spatial signatures can play an important role in tracking progress on initiatives such as the UN's Sustainable Development Goals. Given the rapid urbanisation in the Global South, and the constant retrofitting of cities in the Global North, developing consistent frameworks to characterise cities and track their evolution has never been more important. We hope the present paper contributes in this direction and can be the seed of further discussion and progress on these challenges.

References

- Adjuntament de Barcelona (2018). Estudi del paisatge nocturn de barcelona. Institut del Paisatge Urbà, through 300000Km/s. Available at: https://www.300000kms.net/_arxiv/17082%20paisatge%20nocturn%20memoria.pdf.
- Ahlfeldt, G. M. and Pietrostefani, E. (2019). The economic effects of density: A synthesis. *Journal of Urban Economics*, 111:93–107.
- Alexiou, A., Singleton, A., and Longley, P. A. (2016). A Classification of Multidimensional Open Data for Urban Morphology. *Built Environment*, 42(3):382–395.
- AlSayyad, N. and Roy, A. (2003). *Urban Informality: Transnational Perspectives from the Middle East, Latin America, and South Asia*. Lexington Books.
- Angel, S., Franco, S. A., Liu, Y., and Blei, A. M. (2018). The shape compactness of urban footprints. *Progress in Planning*.
- Araldi, A. and Fusco, G. (2019). From the street to the metropolitan region: Pedestrian perspective in urban fabric analysis:. *Environment and Planning B: Urban Analytics and City Science*, 46(7):1243–1263.
- Arribas-Bel, D. (2014). Accidental, open and everywhere: Emerging data sources for the understanding of cities. *Applied Geography*, 49:45–53.
- Batty, M. and Longley, P. A. (1987). Fractal-based description of urban form. *Environment and Planning B: Planning and Design*, 14(1961):123–134.
- Boarnet, M. G., Crane, R., et al. (2001). *Travel by design: The influence of urban form on travel*. Oxford University Press on Demand.
- Bobkova, E., Berghauser Pont, M., and Marcus, L. (2019). Towards analytical typologies of plot systems: Quantitative profile of five European cities. *Environment and Planning B: Urban Analytics and City Science*, page 239980831988090.
- Boeing, G. (2018). A multi-scale analysis of 27,000 urban street networks: Every US city, town, urbanized area, and Zillow neighborhood. *Environment and Planning B: Urban Analytics and City Science*, 219(4):239980831878459.
- Bondarenko, M., Kerr, D., Sorichetta, A., and Tatem, A. (2020). Census/projection-disaggregated gridded population datasets for 189 countries in 2020 using built-settlement growth model (bsgm) outputs.
- Bourdieu, L., Salat, S., and Nowacki, C. (2012). Assessing cities: A new system of cross-scale spatial indicators. *Building Research & Information*, 40(5):592–605.
- Brenner, N. and Schmid, C. (2015). Towards a new epistemology of the urban? *City*, 19(2-3):151–182.
- Buchhorn, M., Smets, B., Bertels, L., Roo, B. D., Lesiv, M., Tsendlbazar, N.-E., Herold, M., and Fritz, S. (2020). Copernicus Global Land Service: Land Cover 100m: collection 3: epoch 2019: Globe.
- Caniggia, G. and Maffei, G. L. (2001). *Architectural Composition and Building Typology: Interpreting Basic Building*, volume 176. Alinea Editrice, Firenze.

- Carruthers, J. I. and Ulfarsson, G. F. (2003). Urban sprawl and the cost of public services. *Environment and Planning B: Planning and Design*, 30(4):503–522.
- Conzen, M. R. G. (1960). Alnwick, northumberland: a study in town-plan analysis. *Transactions and Papers (Institute of British Geographers)*, (27):iii–122.
- Copernicus Land Monitoring Service (2021). Urban atlas.
- Corbane, C., Politis, P., Kempeneers, P., Simonetti, D., Soille, P., Burger, A., Pesaresi, M., Sabo, F., Syrris, V., and Kemper, T. (2020). A global cloud free pixel- based image composite from sentinel-2 data. *Data in Brief*, 31:105737.
- Defourny, P., Kirches, G., Brockmann, C., Boettcher, M., Peters, M., Bontemps, S., Lamarche, C., Schlerf, M., and Santoro, M. (2012). Land cover cci. *Product User Guide Version*, 2.
- Diamond, D. B. and Tolley, G. S. (2013). *The economics of urban amenities*. Elsevier.
- Dibble, J., Prelorendjos, A., Romice, O., Zanella, M., Strano, E., Pagel, M., and Porta, S. (2019). On the origin of spaces: Morphometric foundations of urban form evolution. *Environment and Planning B: Urban Analytics and City Science*, 46(4):707–730.
- Dibble, J. L. (2016). *Urban morphometrics: towards a quantitative science of urban form*. PhD thesis, University of Strathclyde.
- Duranton, G. and Puga, D. (2020). The economics of urban density. *Journal of Economic Perspectives*, 34(3):3–26.
- EEA, E. (2016). Urban sprawl in europe-joint EEA-FOEN report.
- Elvidge, C. D., Baugh, K. E., Zhizhin, M., and Hsu, F.-C. (2013). Why viirs data are superior to dmsp for mapping nighttime lights. *Proceedings of the Asia-Pacific Advanced Network*, 35(0):62.
- European Environment Agency (1990). CORINE Land Cover. pages 1–163.
- Ewing, R., Hamidi, S., Grace, J. B., and Wei, Y. D. (2016). Does urban sprawl hold down upward mobility? *Landscape and Urban Planning*, 148:80–88.
- Ewing, R. H., Pendall, R., and Chen, D. D. (2002). *Measuring sprawl and its impact*, volume 1. Smart Growth America Washington, DC.
- Filomena, G., Verstegen, J. A., and Manley, E. (2019). A computational approach to ‘The Image of the City’. *Cities*, 89:14–25.
- Fleischmann, M., Feliciotti, A., and Kerr, W. (2021a). Evolution of urban patterns: urban morphology as an open reproducible data science. *Geographical Analysis*.
- Fleischmann, M., Feliciotti, A., Romice, O., and Porta, S. (2020a). Morphological tessellation as a way of partitioning space: Improving consistency in urban morphology at the plot scale. *Computers, Environment and Urban Systems*, 80:101441.
- Fleischmann, M., Feliciotti, A., Romice, O., and Porta, S. (2021b). Methodological foundation of a numerical taxonomy of urban form.
- Fleischmann, M., Romice, O., and Porta, S. (2020b). Measuring urban form: Overcoming terminological inconsistencies for a quantitative and comprehensive morphologic analysis of cities. *Environment and Planning B: Urban Analytics and City Science*, page 2399808320910444.

- Gale, C. G., Singleton, A. D., Bates, A. G., and Longley, P. A. (2016). Creating the 2011 area classification for output areas (2011 oac). *Journal of Spatial Information Science*, 2016(12):1–27.
- Gauthier, P. and Gilliland, J. (2006). Mapping urban morphology: a classification scheme for interpreting contributions to the study of urban form. *Urban morphology*, 10(1):41.
- Geddes, P. (1915). *Cities in evolution: an introduction to the town planning movement and to the study of civics*. London, Williams.
- Georganos, S., Grippa, T., Vanhuysse, S., Lennert, M., Shimoni, M., and Wolff, E. (2018). Very high resolution object-based land use–land cover urban classification using extreme gradient boosting. *IEEE geoscience and remote sensing letters*, 15(4):607–611.
- Gil, J., Montenegro, N., Beirão, J. N., and Duarte, J. P. (2012). On the Discovery of Urban Typologies: Data Mining the Multi-dimensional Character of Neighbourhoods. *Urban Morphology*, 16(1):27–40.
- Glaeser, E. L., Kominers, S. D., Luca, M., and Naik, N. (2018). Big data and big cities: The promises and limitations of improved measures of urban life. *Economic Inquiry*, 56(1):114–137.
- Hamaina, R., Leduc, T., and Moreau, G. (2012). Towards Urban Fabrics Characterization Based on Buildings Footprints. In *Bridging the Geographic Information Sciences*, volume 2, pages 327–346. Springer, Berlin, Heidelberg, Berlin, Heidelberg.
- Harris, R., Sleight, P., and Webber, R. (2005). *Geodemographics, GIS and Neighbourhood Targeting*, volume 8. John Wiley & Sons.
- Hillier, B. (1996). *Space is the machine : a configurational theory of architecture*. Cambridge University Press, Cambridge.
- Homer, C. H., Fry, J. A., and Barnes, C. A. (2012). The national land cover database. *US Geological Survey Fact Sheet*, 3020(4):1–4.
- Horner, M. W. (2004). Exploring metropolitan accessibility and urban structure. *Urban Geography*, 25(3):264–284.
- Hortas-Rico, M. and Solé-Ollé, A. (2010). Does urban sprawl increase the costs of providing local public services? evidence from spanish municipalities. *Urban studies*, 47(7):1513–1540.
- Howarth, P. J. and Boasson, E. (1983). Landsat digital enhancements for change detection in urban environments. *Remote sensing of environment*, 13(2):149–160.
- Jacobs, J. (2016). *The death and life of great American cities*. Vintage.
- Jochem, W. C., Bird, T. J., and Tatem, A. J. (2018). Identifying residential neighbourhood types from settlement points in a machine learning approach. *Computers, Environment and Urban Systems*, 69:104 – 113.
- Jochem, W. C., Leasure, D. R., Pannell, O., Chamberlain, H. R., Jones, P., and Tatem, A. J. (2020). Classifying settlement types from multi-scale spatial patterns of building footprints. *Environment and Planning B: Urban Analytics and City Science*, page 239980832092120.
- Koc, C. B., Osmond, P., Peters, A., and Irger, M. (2017). Mapping local climate zones for urban morphology classification based on airborne remote sensing data. In *2017 Joint Urban Remote Sensing Event (JURSE)*, pages 1–4. IEEE.

- Kohonen, T. (1990). The self-organizing map. *Proceedings of the IEEE*, 78(9):1464–1480.
- Kropf, K. (2009). Aspects of urban form. *Urban Morphology*, 13(2):105–120.
- Kropf, K. (2014). Ambiguity in the definition of built form. *Urban morphology*, 18(1):41–57.
- Kropf, K. (2018). Plots, property and behaviour. *Urban Morphology*, 22(1):1–10.
- Kuffer, M., Pfeffer, K., and Sliuzas, R. (2016). Slums from space-15 years of slum mapping using remote sensing. *Remote Sensing*, 8(6):455.
- Lechner, A. and Blaschke, T. (2019). A Generic Classification Scheme for Urban Structure Types. *Remote Sensing*, 11(2):173.
- Lynch, K. (1960). *The Image of the City*, volume 11. MIT press.
- Mehaffy, M., Porta, S., Rofe, Y., and Salingaros, N. (2010). Urban nuclei and the geometry of streets: The ‘emergent neighborhoods’ model. *Urban Design International*, 15(1):22–46.
- Muratori, S. (1959). Studi per una operante storia urbana di venezia. *Palladio*, 1959:1–113.
- OECD (2018). *Rethinking Urban Sprawl*.
- Oliveira, V. and Yaygin, M. A. (2020). The concept of the morphological region: Developments and prospects. *Urban Morphology*, 24(1):18.
- Openshaw, S. (1981). The modifiable areal unit problem. *Quantitative geography: A British view*, pages 60–69.
- Panerai, P., Castex, J., and Depaule, J.-C. (1997). *Formes urbaines: de l'îlot à la barre*. Editions Parentheses.
- Pauleit, S. and Duhme, F. (2000). Assessing the environmental performance of land cover types for urban planning. *Landscape and urban planning*, 52(1):1–20.
- Pesaresi, M., Florczyk, A., Schiavina, M., Melchiorri, M., and Maffenini, L. (2019). Ghs settlement grid, updated and refined regio model 2014 in application to ghs-built r2018a and ghs-pop r2019a, multitemporal (1975-1990-2000-2015) r2019a. *European Commission, Joint Research Centre (JRC)*.
- Pivo, G. (1993). A taxonomy of suburban office clusters: the case of toronto. *Urban Studies*, 30(1):31–49.
- Porta, S., Crucitti, P., and Latora, V. (2006). The network analysis of urban streets: A primal approach. *Environment and Planning B: Planning and Design*, 33(5):705–725.
- Prasad, S. (2015). *Remotely sensed data characterization, classification, and accuracies*, volume 1.
- Schirmer, P. M. and Axhausen, K. W. (2015). A multiscale classification of urban morphology. *Journal of Transport and Land Use*, 9(1):101–130.
- Schonlau, M. (2002). The clustergram: A graph for visualizing hierarchical and nonhierarchical cluster analyses. *The Stata Journal*, 2(4):391–402.
- Sevtuk, A. and Amindarbari, R. (2020). Does metropolitan form affect transportation sustainability? evidence from us metropolitan areas. *Environment and Planning B: Urban Analytics and City Science*, page 2399808320971310.

- Silva, M., Oliveira, V., and Leal, V. (2017). Urban form and energy demand: A review of energy-relevant urban attributes. *Journal of Planning Literature*, 32(4):346–365.
- Singleton, A. and Arribas-Bel, D. (2021). Geographic data science. *Geographical Analysis*, 53(1):61–75.
- Sneath, P. H., Sokal, R. R., et al. (1973). *Numerical taxonomy. The principles and practice of numerical classification*. Freeman, San Francisco.
- Song, Y. and Knaap, G.-J. (2007). Quantitative Classification of Neighbourhoods: The Neighbourhoods of New Single-family Homes in the Portland Metropolitan Area. *Journal of Urban Design*, 12(1):1–24.
- Song, Y., Popkin, B., and Gordon-Larsen, P. (2013). A national-level analysis of neighborhood form metrics. *Landscape and Urban Planning*, 116:73–85.
- Sorichetta, A., Hornby, G. M., Stevens, F. R., Gaughan, A. E., Linard, C., and Tatem, A. J. (2015). High-resolution gridded population datasets for Latin America and the Caribbean in 2010, 2015, and 2020. *Scientific Data*, 2(1):150045.
- Stark, T., Wurm, M., Zhu, X. X., and Taubenböck, H. (2020). Satellite-based mapping of urban poverty with transfer-learned slum morphologies. *IEEE Journal of Selected Topics in Applied Earth Observations and Remote Sensing*, 13:5251–5263.
- Stewart, I. D. and Oke, T. R. (2012). Local Climate Zones for Urban Temperature Studies. *Bulletin of the American Meteorological Society*, 93(12):1879–1900.
- Taubenböck, H., Debray, H., Qiu, C., Schmitt, M., Wang, Y., and Zhu, X. (2020). Seven city types representing morphologic configurations of cities across the globe. *Cities*, 105:102814.
- Taubenböck, H., Weigand, M., Esch, T., Staab, J., Wurm, M., Mast, J., and Dech, S. (2019). A new ranking of the world's largest cities—do administrative units obscure morphological realities? *Remote Sensing of Environment*, 232:111353.
- Trewartha, G. T. (1934). Japanese cities distribution and morphology. *Geographical Review*, 24(3):404–417.
- Usui, H. and Asami, Y. (2013). Estimation of mean lot depth and its accuracy. *Journal of City Planning Institute of Japan*, 48(3):357–362.
- Venerandi, A., Fusco, G., Tettamanzi, A., and Emsellem, D. (2019). A machine learning approach to study the relationship between features of the urban environment and street value. *Urban Science*, 3(3):100.
- Venerandi, A., Quattrone, G., and Capra, L. (2018). A scalable method to quantify the relationship between urban form and socio-economic indexes. *EPJ Data Science*, 7:1–21.
- Webber, R. and Burrows, R. (2018). *The Predictive Postcode: The Geodemographic Classification of British Society*. Sage.
- Wei, L., Luo, Y., Wang, M., Cai, Y., Su, S., Li, B., and Ji, H. (2020). Multiscale identification of urban functional polycentricity for planning implications: An integrated approach using geo-big transport data and complex network modeling. *Habitat International*, 97:102134.
- Weng, Q. and Quattrochi, D. A. (2018). *Urban remote sensing*. CRC press.
- Zheng, Y., Capra, L., Wolfson, O., and Yang, H. (2014). Urban computing: concepts, methodologies, and applications. *ACM Transactions on Intelligent Systems and Technology (TIST)*, 5(3):1–55.

Appendix A. Technical appendix

A. The complete lists of used characters reflecting both form and function across case studies

A..1 Barcelona

The data for the Barcelona case study has been retrieved from the Barcelona's City Hall Open Data Service Open Data BCN available at opendata-ajuntament.barcelona.cat, OpenStreetMap, and Spanish Cadastre available at catastro.minhap.es. The data represents versions available on December 01, 2020.

Table 3: The complete list of form characters used in the Barcelona case study. The implementation details are available in Jupyter notebooks available at [janonymised](#) for peer-review. Characters are adapted to enclosed tessellation from Fleischmann et al. (2021b).

index	element	context	category
area	building	building	dimension
perimeter	building	building	dimension
courtyard area	building	building	dimension
circular compactness	building	building	shape
corners	building	building	shape
squareness	building	building	shape
equivalent rectangular index	building	building	shape
elongation	building	building	shape
centroid - corner distance deviation	building	building	shape
centroid - corner mean distance	building	building	dimension
solar orientation	building	building	distribution
street alignment	building	building	distribution
cell alignment	building	building	distribution
longest axis length	tessellation cell	tessellation cell	dimension
area	tessellation cell	tessellation cell	dimension
circular compactness	tessellation cell	tessellation cell	shape
equivalent rectangular index	tessellation cell	tessellation cell	shape
solar orientation	tessellation cell	tessellation cell	distribution
coverage area ratio	tessellation cell	tessellation cell	intensity
street alignment	tessellation cell	tessellation cell	distribution
length	street segment	street segment	dimension
width	street profile	street segment	dimension
openness	street profile	street segment	distribution
width deviation	street profile	street segment	diversity
linearity	street segment	street segment	shape
area covered	street segment	street segment	dimension
buildings per meter	street segment	street segment	intensity
area covered	street node	street node	dimension

Continued on next page

index	element	context	category
alignment	neighbouring buildings	neighbouring (queen)	cells distribution
mean distance	neighbouring buildings	neighbouring (queen)	cells distribution
weighted neighbours	tessellation cell	neighbouring (queen)	cells distribution
area covered	neighbouring cells	neighbouring (queen)	cells dimension
reached area	neighbouring segments	neighbouring segments	dimension
reached cells	neighbouring segments	neighbouring segments	intensity
degree	street node	neighbouring nodes	distribution
mean distance to neighbouring nodes	street node	neighbouring nodes	dimension
shared walls ratio	adjacent buildings	adjacent buildings	distribution
mean inter-building distance	neighbouring buildings	cell queen neighbours 3	distribution
weighted reached enclosures	neighbouring tessellation cells	cell queen neighbours 3	intensity
area	enclosure	enclosure	dimension
perimeter	enclosure	enclosure	dimension
circular compactness	enclosure	enclosure	shape
equivalent rectangular index	enclosure	enclosure	shape
compactness-weighted axis	enclosure	enclosure	shape
solar orientation	enclosure	enclosure	distribution
weighted neighbours	enclosure	enclosure	distribution
weighted cells	enclosure	enclosure	intensity
local meshedness	street network	nodes 5 steps	connectivity
mean segment length	street network	segment 3 steps	dimension
cul-de-sac length	street network	nodes 3 steps	dimension
node density	street network	nodes 5 steps	intensity
proportion of cul-de-sacs	street network	nodes 5 steps	connectivity
proportion of 3-way intersections	street network	nodes 5 steps	connectivity
proportion of 4-way intersections	street network	nodes 5 steps	connectivity
degree weighted node density	street network	nodes 5 steps	intensity
local closeness centrality	street network	nodes 5 steps	connectivity
perimeter wall length	adjacent buildings	joined buildings	dimension
number of courtyards	adjacent buildings	joined buildings	intensity
square clustering	street network	street network	connectivity

Table 4: The complete list of function characters and transfer methods used in the Barcelona case study. The implementation details are available in Jupyter notebooks available at [janonymised for peer-review](#).

character	input spatial unit	transfer method
population	block	Building-based mapping Dasymetric
number of car parks	block	Dasymetric mapping
number of other items that are not premises	block	Dasymetric mapping
land use	parcel	Spatial join (centroid)
number of dwellings	building	Attribute join
current use	building	Attribute join
age	building	Attribute join
heritage	points	Accessibility - # within 15min
heritage	polygons	Spatial join
culture (cinemas, museums, libraries, theaters)	points	Accessibility - distance to nearest / # within 15min
parks	points	Accessibility - distance to nearest / # within 15min
economic census	poitnts	Accessibility - distance to nearest / # within 15min
restaurants	point	Accessibility - distance to nearest / # within 15min
trees	points	Spatial join (count)
NDVI	raster 1m	Zonal stats

A.2 Medellin

The data for the Medellin case study has been retrieved from the GeoMedellin Open Data portal available at medellin.gov.co/geomedellin/, OpenStreetMap, WorldPop gridded population estimates (Bondarenko et al., 2020), and a Sentinel 2 cloud-free composite (Corbane et al., 2020). The data represents versions available on January 05, 2021.

Table 5: The complete list of form characters used in the Medellin case study. The implementation details are available in Jupyter notebooks available at [janonymised for peer-review](#). Characters are adapted to enclosed tessellation from Fleischmann et al. (2021b).

index	element	context	category
area	building	building	dimension
perimeter	building	building	dimension
courtyard area	building	building	dimension
circular compactness	building	building	shape
corners	building	building	shape
squareness	building	building	shape
equivalent rectangular index	building	building	shape

Continued on next page

index	element	context	category
elongation	building	building	shape
centroid - corner distance deviation	building	building	shape
centroid - corner mean distance	building	building	dimension
solar orientation	building	building	distribution
street alignment	building	building	distribution
cell alignment	building	building	distribution
longest axis length	tessellation cell	tessellation cell	dimension
area	tessellation cell	tessellation cell	dimension
circular compactness	tessellation cell	tessellation cell	shape
equivalent rectangular index	tessellation cell	tessellation cell	shape
solar orientation	tessellation cell	tessellation cell	distribution
coverage area ratio	tessellation cell	tessellation cell	intensity
street alignment	tessellation cell	tessellation cell	distribution
length	street segment	street segment	dimension
width	street profile	street segment	dimension
openness	street profile	street segment	distribution
width deviation	street profile	street segment	diversity
linearity	street segment	street segment	shape
area covered	street segment	street segment	dimension
buildings per meter	street segment	street segment	intensity
area covered	street node	street node	dimension
alignment	neighbouring buildings	neighbouring (queen)	cells distribution
mean distance	neighbouring buildings	neighbouring (queen)	cells distribution
weighted neighbours	tessellation cell	neighbouring (queen)	cells distribution
area covered	neighbouring cells	neighbouring (queen)	cells dimension
reached area	neighbouring segments	neighbouring segments	dimension
reached cells	neighbouring segments	neighbouring segments	intensity
degree	street node	neighbouring nodes	distribution
mean distance to neighbouring nodes	street node	neighbouring nodes	dimension
shared walls ratio	adjacent buildings	adjacent buildings	distribution
mean inter-building distance	neighbouring buildings	cell queen neighbours 3	distribution
weighted reached enclosures	neighbouring tessellation cells	cell queen neighbours 3	intensity
area	enclosure	enclosure	dimension
perimeter	enclosure	enclosure	dimension
circular compactness	enclosure	enclosure	shape
equivalent rectangular index	enclosure	enclosure	shape

Continued on next page

index	element	context	category
compactness-weighted axis	enclosure	enclosure	shape
solar orientation	enclosure	enclosure	distribution
weighted neighbours	enclosure	enclosure	distribution
weighted cells	enclosure	enclosure	intensity
local meshedness	street network	nodes 5 steps	connectivity
mean segment length	street network	segment 3 steps	dimension
cul-de-sac length	street network	nodes 3 steps	dimension
node density	street network	nodes 5 steps	intensity
proportion of cul-de-sacs	street network	nodes 5 steps	connectivity
proportion of 3-way intersections	street network	nodes 5 steps	connectivity
proportion of 4-way intersections	street network	nodes 5 steps	connectivity
degree weighted node density	street network	nodes 5 steps	intensity
local closeness centrality	street network	nodes 5 steps	connectivity
perimeter wall length	adjacent buildings	joined buildings	dimension
number of courtyards	adjacent buildings	joined buildings	intensity
square clustering	street network	street network	connectivity

Table 6: The complete list of function characters and transfer methods used in the Medellin case study. The implementation details are available in Jupyter notebooks available at [janonymised for peer-review](#).

character	input spatial unit	transfer method
trees	points	Spatial join (count)
parks	polygons	Distance to nearest
heritage large areas	polygons	Spatial join (boolean)
land use	polygons	tobler
points of interest	points	Accessibility - distance to nearest / # within 15min
public spaces	polygons	Accessibility - area within radius
population	raster	Zonal stats
NDVI	raster	Zonal stats

A..3 Dar es Salaam

The data for the Dar es Salaam case study has been retrieved from [OpenStreetMap](#), WorldPop gridded population estimates (Bondarenko et al., 2020), a Copernicus Global Land Cover (Buchhorn et al., 2020), VIIRS Night lights data (June 2020) (Elvidge et al., 2013), and a Sentinel 2 cloud-free composite (Corbane et al., 2020). The data represents versions available on December 18, 2020.

Table 7: The complete list of form characters used in the Dar es Salaam case study. The implementation details are available in Jupyter notebooks available at [janonymised](#) for peer-review. Characters are adapted to enclosed tessellation from Fleischmann et al. (2021b).

index	element	context	category
area	building	building	dimension
perimeter	building	building	dimension
courtyard area	building	building	dimension
circular compactness	building	building	shape
corners	building	building	shape
squareness	building	building	shape
equivalent rectangular index	building	building	shape
elongation	building	building	shape
centroid - corner distance deviation	building	building	shape
centroid - corner mean distance	building	building	dimension
solar orientation	building	building	distribution
street alignment	building	building	distribution
cell alignment	building	building	distribution
longest axis length	tessellation cell	tessellation cell	dimension
area	tessellation cell	tessellation cell	dimension
circular compactness	tessellation cell	tessellation cell	shape
equivalent rectangular index	tessellation cell	tessellation cell	shape
solar orientation	tessellation cell	tessellation cell	distribution
coverage area ratio	tessellation cell	tessellation cell	intensity
length	street segment	street segment	dimension
width	street profile	street segment	dimension
openness	street profile	street segment	distribution
width deviation	street profile	street segment	diversity
linearity	street segment	street segment	shape
area covered	street segment	street segment	dimension
buildings per meter	street segment	street segment	intensity
area covered	street node	street node	dimension
alignment	neighbouring buildings	neighbouring (queen)	cells distribution
mean distance	neighbouring buildings	neighbouring (queen)	cells distribution
weighted neighbours	tessellation cell	neighbouring (queen)	cells distribution
area covered	neighbouring cells	neighbouring (queen)	cells dimension
reached cells	neighbouring segments	neighbouring segments	intensity
reached area	neighbouring segments	neighbouring segments	dimension
degree	street node	neighbouring nodes	distribution

Continued on next page

index	element	context	category
mean distance to neighbouring nodes	street node	neighbouring nodes	dimension
mean inter-building distance weighted reached enclosures	neighbouring buildings neighbouring tessellation cells	cell queen neighbours 3 cell queen neighbours 3	distribution intensity
reached neighbors	neighbouring tessellation cells	cell queen neighbours 3	intensity
reached area	neighbouring tessellation cells	cell queen neighbours 3	dimension
area	enclosure	enclosure	dimension
perimeter	enclosure	enclosure	dimension
circular compactness	enclosure	enclosure	shape
equivalent rectangular index	enclosure	enclosure	shape
compactness-weighted axis	enclosure	enclosure	shape
solar orientation	enclosure	enclosure	distribution
weighted neighbours	enclosure	enclosure	distribution
weighted cells	enclosure	enclosure	intensity
local meshedness	street network	nodes 5 steps	connectivity
mean segment length	street network	segment 3 steps	dimension
cul-de-sac length	street network	nodes 3 steps	dimension
reached area	street network	segment 3 steps	dimension
reached cells	street network	segment 3 steps	intensity
node density	street network	nodes 5 steps	intensity
proportion of cul-de-sacs	street network	nodes 5 steps	connectivity
proportion of 3-way intersections	street network	nodes 5 steps	connectivity
proportion of 4-way intersections	street network	nodes 5 steps	connectivity
degree weighted node density	street network	nodes 5 steps	intensity
local closeness centrality	street network	nodes 5 steps	connectivity
square clustering	street network	street network	connectivity

Table 8: The complete list of function characters and transfer methods used in the Dar es Salaam case study. The implementation details are available in Jupyter notebooks available at [janonymised for peer-review](#).

character	input spatial unit	transfer method
population	raster 100m	Zonal stats
NDVI	raster 10m	Zonal stats
land cover	raster	Zonal stats
night lights	raster	Zonal stats

A..4 Houston

The data for the Houston case study has been retrieved from [OpenStreetMap](https://www.openstreetmap.org), Microsoft Building Footprints available from microsoft.com/en-us/maps/building-footprints, WorldPop gridded population estimates (Bondarenko et al., 2020), a Copernicus Global Land Cover (Buchhorn et al., 2020), VIIRS Night lights data (November 2019) (Elvidge et al., 2013), a Sentinel 2 cloud-free composite (Corbane et al., 2020), and the Longitudinal Employer-Household Dynamics data from US Census 2011 available from lehd.ces.census.gov/data/. The data represents versions available on January 13, 2021.

Table 9: The complete list of form characters used in the Houston case study. The implementation details are available in Jupyter notebooks available at [janonymised for peer-review](#). Characters are adapted to enclosed tessellation from Fleischmann et al. (2021b).

index	element	context	category
area	building	building	dimension
perimeter	building	building	dimension
courtyard area	building	building	dimension
circular compactness	building	building	shape
corners	building	building	shape
squareness	building	building	shape
equivalent rectangular index	building	building	shape
elongation	building	building	shape
centroid - corner distance deviation	building	building	shape
centroid - corner mean distance	building	building	dimension
solar orientation	building	building	distribution
street alignment	building	building	distribution
cell alignment	building	building	distribution
longest axis length	tessellation cell	tessellation cell	dimension
area	tessellation cell	tessellation cell	dimension
circular compactness	tessellation cell	tessellation cell	shape
equivalent rectangular index	tessellation cell	tessellation cell	shape
solar orientation	tessellation cell	tessellation cell	distribution
coverage area ratio	tessellation cell	tessellation cell	intensity
length	street segment	street segment	dimension
width	street profile	street segment	dimension
openness	street profile	street segment	distribution
width deviation	street profile	street segment	diversity
linearity	street segment	street segment	shape
area covered	street segment	street segment	dimension
buildings per meter	street segment	street segment	intensity
alignment	neighbouring buildings	neighbouring (queen)	cells
mean distance	neighbouring buildings	neighbouring (queen)	cells
			distribution

Continued on next page

index	element	context	category
weighted neighbours	tessellation cell	neighbouring (queen)	cells distribution
area covered	neighbouring cells	neighbouring (queen)	cells dimension
reached cells	neighbouring segments	neighbouring segments	intensity
reached area	neighbouring segments	neighbouring segments	dimension
degree	street node	neighbouring nodes	distribution
mean distance to neighbouring nodes	street node	neighbouring nodes	dimension
mean inter-building distance	neighbouring buildings	cell queen neighbours 3	distribution
weighted reached enclosures	neighbouring tessellation cells	cell queen neighbours 3	intensity
reached neighbors	neighbouring tessellation cells	cell queen neighbours 3	intensity
reached area	neighbouring tessellation cells	cell queen neighbours 3	dimension
area	enclosure	enclosure	dimension
perimeter	enclosure	enclosure	dimension
circular compactness	enclosure	enclosure	shape
equivalent rectangular index	enclosure	enclosure	shape
compactness-weighted axis	enclosure	enclosure	shape
solar orientation	enclosure	enclosure	distribution
weighted neighbours	enclosure	enclosure	distribution
weighted cells	enclosure	enclosure	intensity
local meshedness	street network	nodes 5 steps	connectivity
mean segment length	street network	segment 3 steps	dimension
cul-de-sac length	street network	nodes 3 steps	dimension
reached area	street network	segment 3 steps	dimension
reached cells	street network	segment 3 steps	intensity
node density	street network	nodes 5 steps	intensity
proportion of cul-de-sacs	street network	nodes 5 steps	connectivity
proportion of 3-way intersections	street network	nodes 5 steps	connectivity
proportion of 4-way intersections	street network	nodes 5 steps	connectivity
degree weighted node density	street network	nodes 5 steps	intensity
local closeness centrality	street network	nodes 5 steps	connectivity
square clustering	street network	street network	connectivity

Table 10: The complete list of function characters and transfer methods used in the Houston case study. The implementation details are available in Jupyter notebooks available at [janonymised](#) for peer-review.

character	input spatial unit	transfer method
population	raster 100m	Zonal stats
NDVI	raster 10m	Zonal stats
land cover	raster	Zonal stats
night lights	raster	Zonal stats
employment	census block	Dasymetric interpolation
historical sites	point	Accessibility

A.5 Singapore

The data for the Singapore case study has been retrieved from [OpenStreetMap](#), Singapore Open data portal available at [data.gov.sg](#), WorldPop gridded population estimates (Bondarenko et al., 2020), VIIRS Night lights data (November 2019) (Elvidge et al., 2013), and a Sentinel 2 cloud-free composite (Corbane et al., 2020). The data represents versions available on February 1, 2021.

Table 11: The complete list of form characters used in the Singapore case study. The implementation details are available in Jupyter notebooks available at [janonymised](#) for peer-review. Characters are adapted to enclosed tessellation from [Fleischmann et al. \(2021b\)](#).

index	element	context	category
area	building	building	dimension
perimeter	building	building	dimension
courtyard area	building	building	dimension
circular compactness	building	building	shape
corners	building	building	shape
squareness	building	building	shape
equivalent rectangular index	building	building	shape
elongation	building	building	shape
centroid - corner distance deviation	building	building	shape
centroid - corner mean distance	building	building	dimension
solar orientation	building	building	distribution
street alignment	building	building	distribution
cell alignment	building	building	distribution
longest axis length	tessellation cell	tessellation cell	dimension
area	tessellation cell	tessellation cell	dimension
circular compactness	tessellation cell	tessellation cell	shape
equivalent rectangular index	tessellation cell	tessellation cell	shape
solar orientation	tessellation cell	tessellation cell	distribution
coverage area ratio	tessellation cell	tessellation cell	intensity
street alignment	tessellation cell	tessellation cell	distribution
length	street segment	street segment	dimension

Continued on next page

index	element	context	category
width	street profile	street segment	dimension
openness	street profile	street segment	distribution
width deviation	street profile	street segment	diversity
linearity	street segment	street segment	shape
area covered	street segment	street segment	dimension
buildings per meter	street segment	street segment	intensity
area covered	street node	street node	dimension
alignment	neighbouring buildings	neighbouring (queen)	cells distribution
mean distance	neighbouring buildings	neighbouring (queen)	cells distribution
weighted neighbours	tessellation cell	neighbouring (queen)	cells distribution
area covered	neighbouring cells	neighbouring (queen)	cells dimension
reached area	neighbouring segments	neighbouring segments	dimension
reached cells	neighbouring segments	neighbouring segments	intensity
degree	street node	neighbouring nodes	distribution
mean distance to neighbouring nodes	street node	neighbouring nodes	dimension
shared walls ratio	adjacent buildings	adjacent buildings	distribution
mean inter-building distance	neighbouring buildings	cell queen neighbours 3	distribution
weighted reached enclosures	neighbouring tessellation cells	cell queen neighbours 3	intensity
area	enclosure	enclosure	dimension
perimeter	enclosure	enclosure	dimension
circular compactness	enclosure	enclosure	shape
equivalent rectangular index	enclosure	enclosure	shape
compactness-weighted axis	enclosure	enclosure	shape
solar orientation	enclosure	enclosure	distribution
weighted neighbours	enclosure	enclosure	distribution
weighted cells	enclosure	enclosure	intensity
local meshedness	street network	nodes 5 steps	connectivity
mean segment length	street network	segment 3 steps	dimension
cul-de-sac length	street network	nodes 3 steps	dimension
node density	street network	nodes 5 steps	intensity
proportion of cul-de-sacs	street network	nodes 5 steps	connectivity
proportion of 3-way intersections	street network	nodes 5 steps	connectivity
proportion of 4-way intersections	street network	nodes 5 steps	connectivity
degree weighted node density	street network	nodes 5 steps	intensity
local closeness centrality	street network	nodes 5 steps	connectivity

Continued on next page

index	element	context	category
perimeter wall length	adjacent buildings	joined buildings	dimension
number of courtyards	adjacent buildings	joined buildings	intensity
square clustering	street network	street network	connectivity

Table 12: The complete list of function characters and transfer methods used in the Singapore case study. The implementation details are available in Jupyter notebooks available at [janonymised](#) for peer-review.

character	input spatial unit	transfer method
NDVI	raster	Zonal stats
population	raster	Zonal stats
night lights	raster	Zonal stats
eating est	point	Accessibility
supermarkets	point	Accessibility
land use	polygon	Areal interpolation
parks	point	Accessibility
monuments	point	Accessibility

B. Clustergrams

C. Summary values per cluster

D. Proportion of ET cells belonging to individual clusters

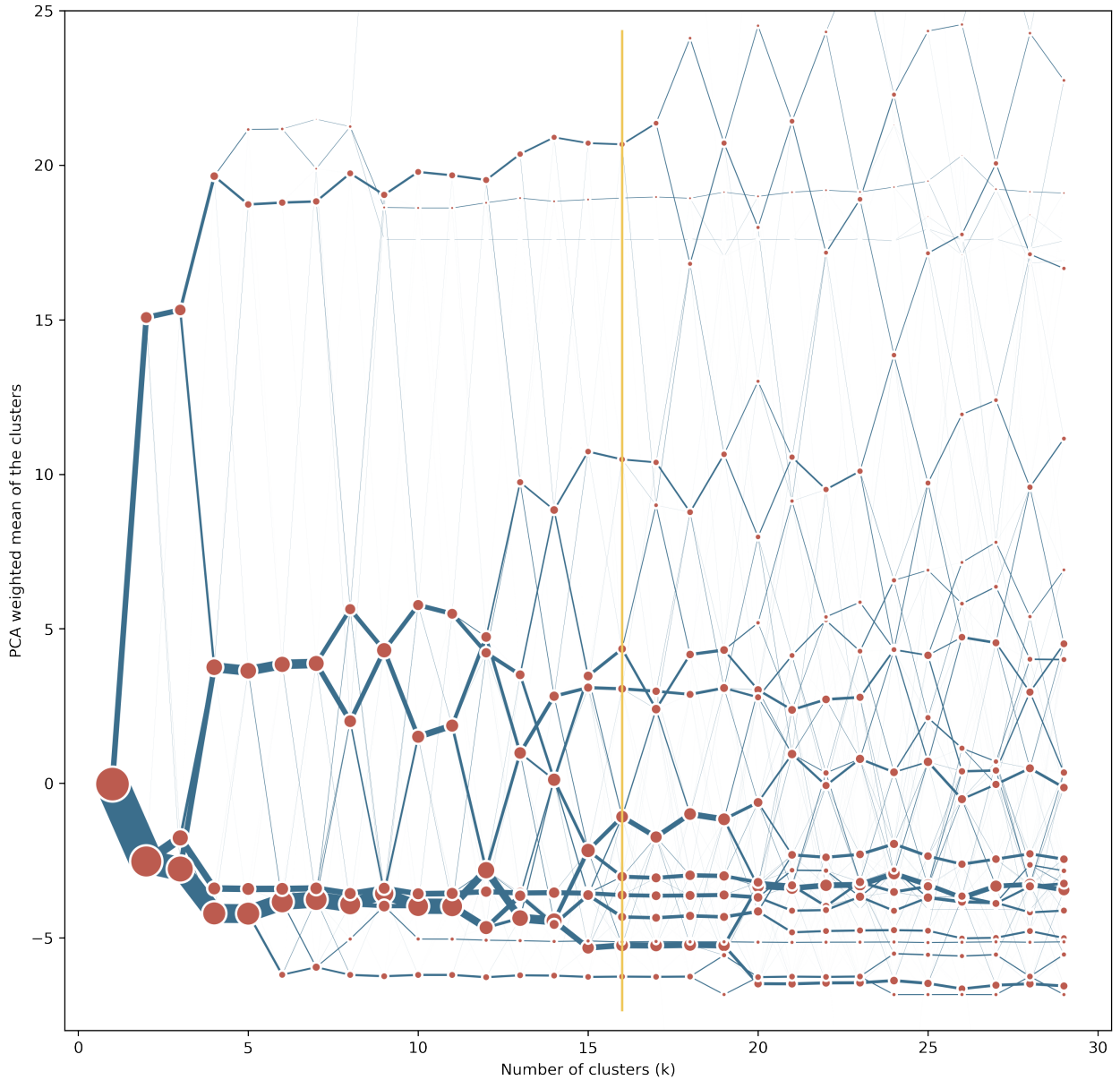


Figure 6: Clustergram (truncated along the vertical axis) illustrating the behaviour of dataset in different clustering options. The result suggests two different solutions, a (very) conservative one with 4 classes and the other with 16 classes. For the purpose of spatial signatures, it is more suitable a solution with more classes providing more detailed classification. Therefore, we select 16 classes.

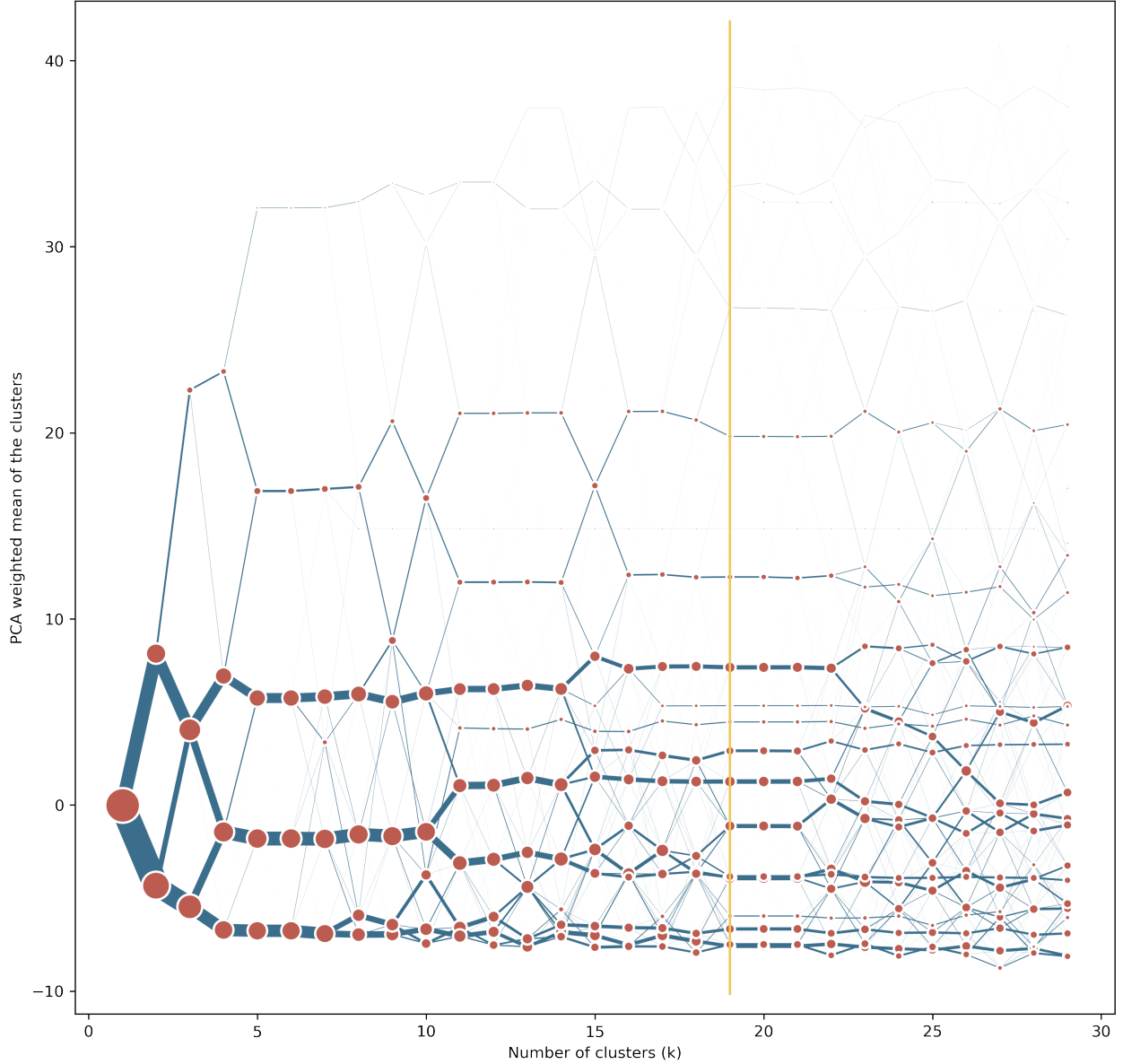


Figure 7: Clustergram (truncated along the vertical axis) illustrating the behaviour of dataset in different clustering options. The result suggests 3 different solutions, a (very) conservative one with 4 classes, middle option with 11 classes and the detailed one with 19 classes. For the purpose of spatial signatures, it is more suitable a solution with more classes providing more detailed classification. Therefore, we select 19 classes.

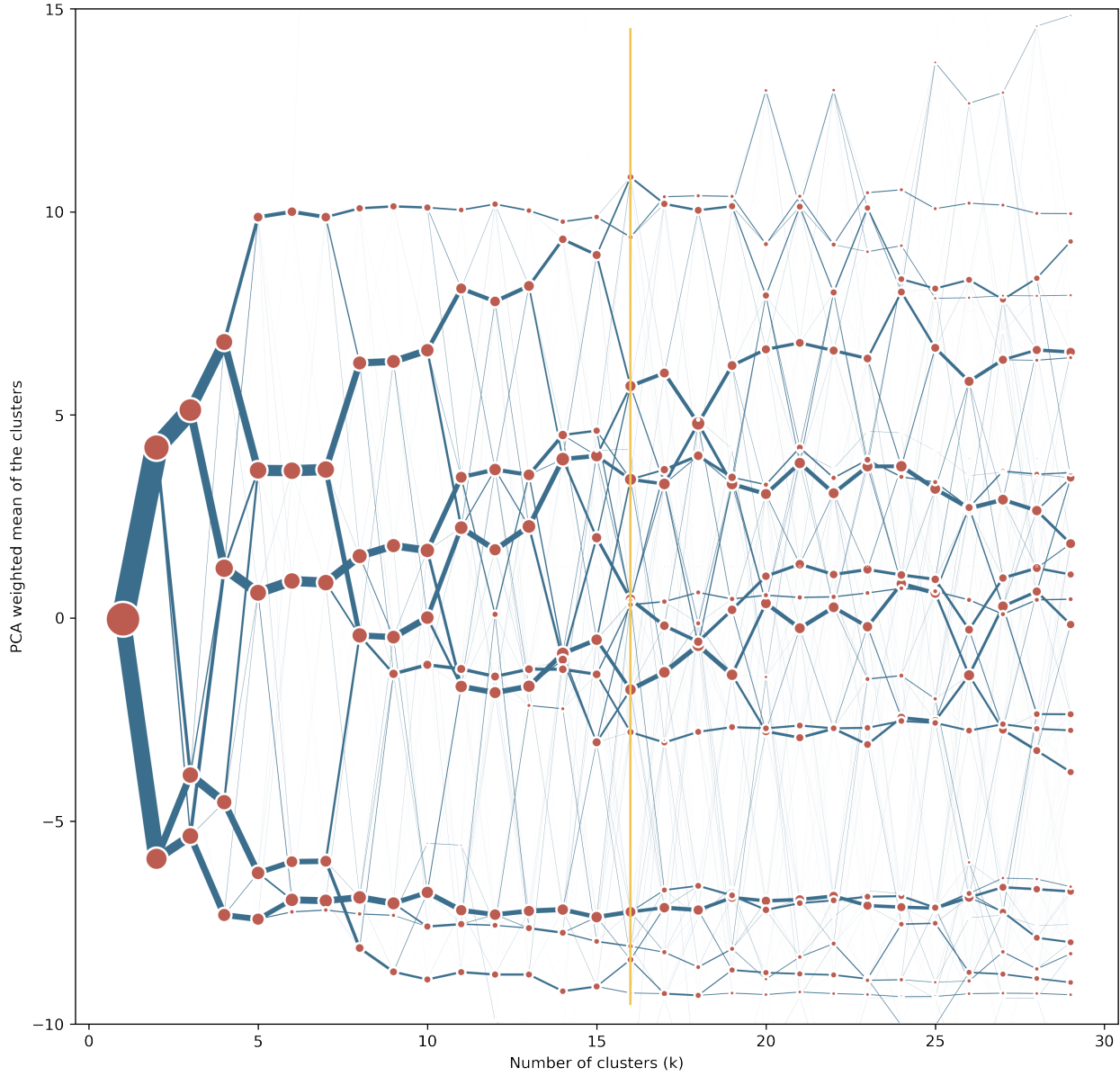


Figure 8: Clustergram (truncated along the vertical axis) illustrating the behaviour of dataset in different clustering options. The result suggests 3 different solutions, a conservative one with 4 classes, middle option with 8 classes and the detailed one with 16 classes. For the purpose of spatial signatures, it is more suitable a solution with more classes providing more detailed classification. Therefore, we select 16 classes.

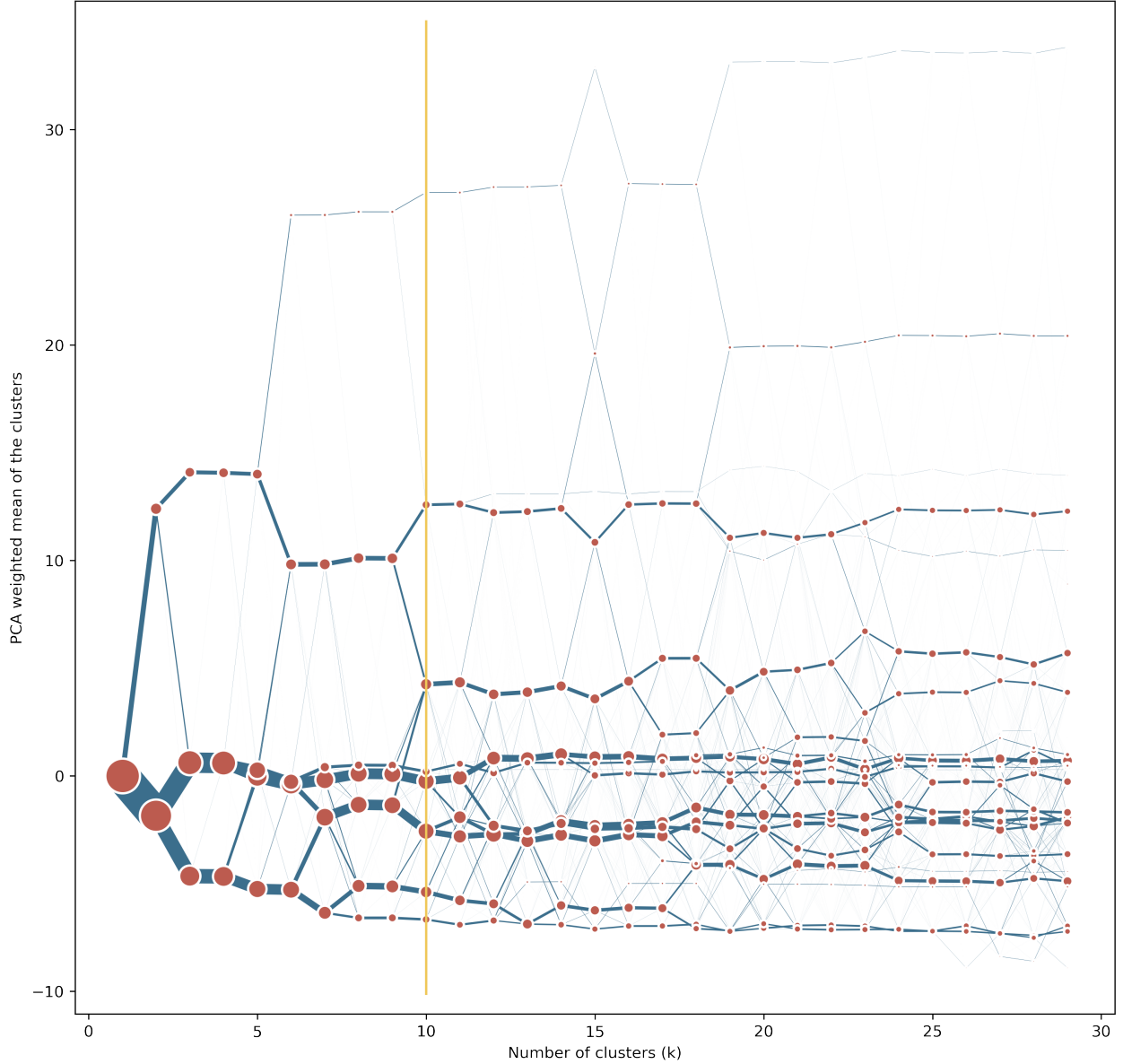


Figure 9: Clustergram (truncated along the vertical axis) illustrating the behaviour of dataset in different clustering options. The result suggests 3 different solutions, a (very) conservative one with 3 classes, middle option with 6 classes and the detailed one with 10 classes. For the purpose of spatial signatures, it is more suitable a solution with more classes providing more detailed classification. Therefore, we select 10 classes.

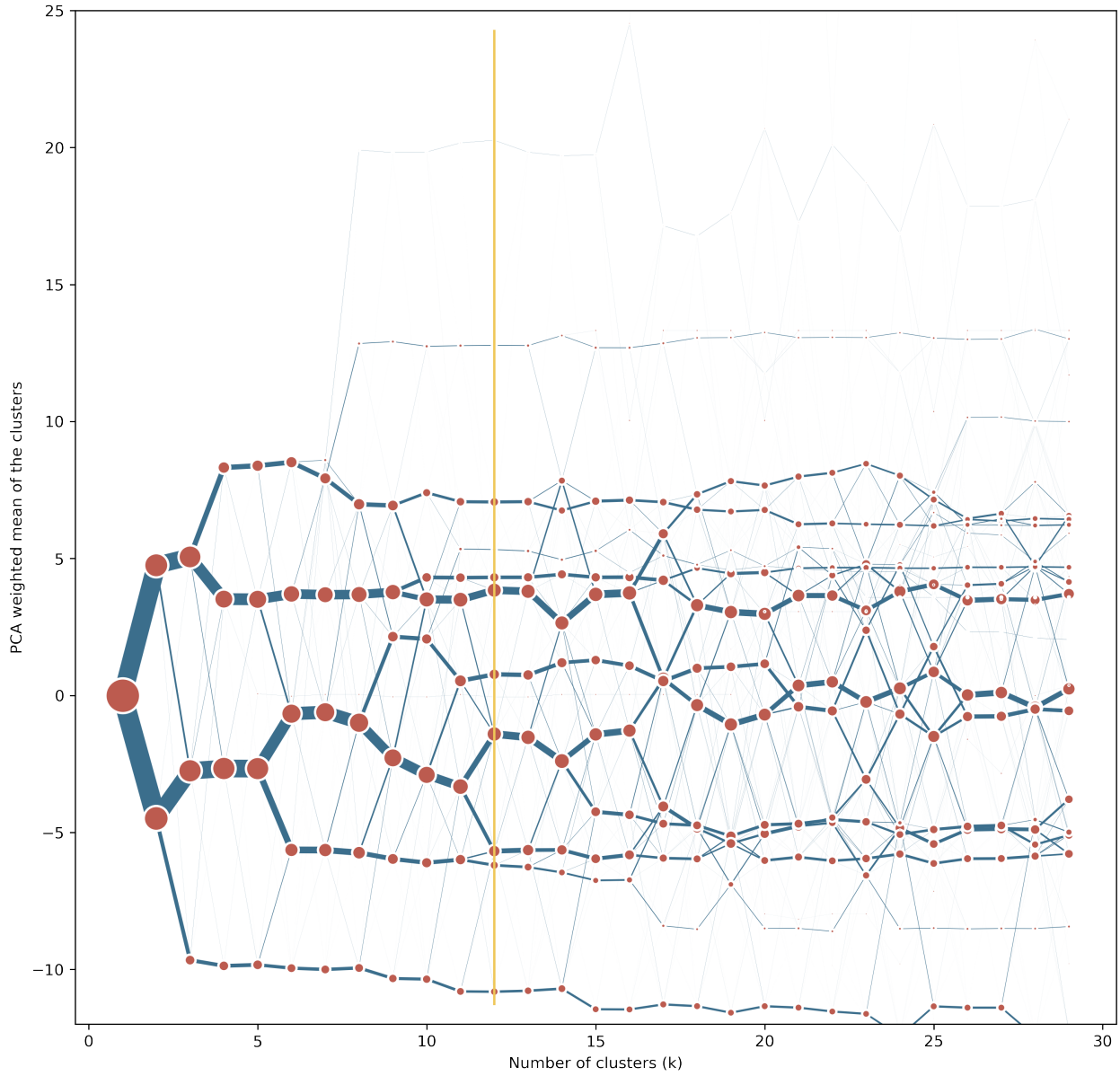


Figure 10: Clustergram (truncated along the vertical axis) illustrating the behaviour of dataset in different clustering options. The result suggests 3 different solutions, a (very) conservative one with 3 classes, middle option with 6 classes and the detailed one with 12 classes. For the purpose of spatial signatures, it is more suitable a solution with more classes providing more detailed classification. Therefore, we select 12 classes.

	Neighbourhoods on steep slopes		Patchy grids		Rigid planned grid		Granular neighbourhoods		Transitional grid		Detached areas		Industrial pockets		Urban periphery		Historical neighbourhoods		Port development		Green urban hills		Industrial development		Medieval city		Heterogeneous dense neighbourhoods		Planned small-scale grid		Industrial zones				
orientation of ETC	22.71	23.87	41.32	34.67	36.97	16.92	24.14	23.26	12.14	9.43	26.67	24.91	33.16	30.86	16.46	24.10																			
orientation of building	22.78	24.14	41.52	35.39	37.44	24.40	24.91	23.63	11.51	9.85	28.54	23.85	33.49	31.60	16.40	24.74																			
cell alignment of building	5.91	3.62	2.47	2.31	2.82	10.87	10.66	10.54	2.70	0.70	8.14	9.48	2.19	4.05	0.51	4.63																			
longest axis length of ETC	36.34	42.13	47.21	27.77	41.66	572.94	26.66	72.83	28.06	145.90	82.95	33.97	30.99	71.93	23.20	173.25																			
area of ETC	694.61	845.98	784.38	279.04	719.04	102133.64	359.73	3271.29	286.56	5331.61	4502.30	1068.87	408.86	2459.21	378.99	9359.05																			
circular compactness of ETC	0.42	0.42	0.39	0.41	0.41	0.37	0.48	0.42	0.38	0.37	0.44	0.55	0.43	0.44	0.53	0.38																			
equivalent rectangular index of ETC	0.94	0.94	0.94	0.94	0.94	0.90	0.99	0.94	0.94	1.00	0.95	1.01	0.92	0.95	0.98	0.92																			
covered area ratio of ETC	0.41	0.53	0.58	0.63	0.57	0.24	0.20	0.16	0.62	0.41	0.57	16.83	0.74	0.38	0.56	58.62																			
alignment of neighbouring buildings	5.18	4.64	3.69	1.85	4.03	6.91	9.25	9.57	2.09	0.30	6.70	11.03	4.15	4.04	0.59	2.85																			
mean distance between neighbouring buildings	9.42	7.13	4.76	2.59	5.27	90.19	9.09	30.94	3.00	4.35	31.33	9.78	2.32	16.99	3.60	36.78																			
perimeter-weighted neighbours of ETC	0.07	0.05	0.04	0.07	0.05	0.04	0.10	0.05	0.07	0.00	0.04	0.10	0.07	0.04	0.09	0.03																			
area covered by neighbouring cells	6795.80	7702.87	5311.82	1898.25	5414.29	529126.73	197455.45	28918.23	23393.73	548779.83	501674.44	21093.12	3956.47	21400.12	3829.02	168892.16																			
mean inter-building distance	17.17	11.31	7.89	4.21	8.90	90.87	19.30	52.47	5.92	2.56	43.64	11.38	4.12	24.36	8.78	54.15																			
street alignment of ETC	8.84	5.13	2.49	3.20	3.50	10.86	13.31	13.12	3.80	3.63	9.35	3.21	4.83	4.54	1.11	6.13																			
weighted reached enclosures of ETC	0.00	0.00	0.00	0.00	0.00	0.00	0.00	0.00	0.00	0.00	0.00	0.00	0.00	0.00	0.00	0.00																			
area of building	148.58	359.40	402.37	16.86	341.77	19107.75	81.55	117.90	158.42	23.30	894.47	1141.58	288.17	706.72	191.41	1981.10																			
perimeter of building	53.71	82.80	98.19	59.93	85.96	743.97	27.86	44.67	56.10	243.10	107.85	108.34	78.85	117.83	46.65	965.17																			
courtyard area of building	1.71	15.99	8.52	2.09	6.26	5680.19	0.00	0.54	1.42	0.00	347.51	2534.40	14.10	22.81	0.93	20899.38																			
circular compactness of building	0.47	0.45	0.43	0.44	0.44	0.55	0.76	0.51	0.41	0.40	0.47	0.88	0.43	0.46	0.55	0.45																			
corners of building	7.90	8.76	9.82	7.13	9.00	12.31	11.58	7.72	6.49	16.00	10.10	23.36	10.03	10.31	5.96	16.36																			
squareness of building	6.84	7.60	7.30	3.96	6.54	15.94	44.12	7.58	5.06	0.32	7.02	6.16	9.38	6.60	1.46	6.97																			
equivalent rectangular index of building	0.91	0.88	0.86	0.91	0.87	0.91	1.06	0.94	0.93	0.91	0.90	1.09	0.83	0.88	0.95	0.92																			
elongation of building	0.59	0.56	0.53	0.51	0.55	0.70	0.80	0.68	0.47	0.46	0.63	0.91	0.55	0.59	0.73	0.54																			
centroid - corner mean distance of building	7.67	11.19	13.15	8.85	11.69	64.42	4.72	6.62	8.86	28.17	11.85	8.34	9.56	16.08	7.16	56.77																			
centroid - corner distance deviation of building	1.51	2.23	2.61	1.56	2.28	36.43	0.23	1.19	1.44	13.49	2.76	0.98	2.59	2.73	0.87	14.40																			
shared walls ratio of buildings	0.28	0.41	0.49	0.49	0.45	0.04	0.04	0.05	0.53	0.00	0.10	0.05	0.52	0.24	0.54	0.79																			
length of contiguous perimeter wall	292.95	542.61	446.00	385.06	401.49	2354.52	323.21	58.03	431.24	243.14	260.35	1304.11	482.57	368.66	389.03	3067.69																			
street alignment of building	7.96	5.19	2.67	2.49	3.61	14.84	11.90	12.62	2.98	3.21	8.50	8.60	4.99	4.52	1.13	4.30																			
number of courtyards	8.61	16.11	35.84	19.90	23.31	2.50	1.13	0.10	14.74	0.00	1.07	4.87	30.32	6.72	3.53	11.48																			
length of street segment	142.68	101.28	131.66	88.42	111.28	481.27	389.72	273.89	87.98	441.35	176.99	291.48	71.29	142.28	67.69	406.80																			
width of street profile	18.23	17.40	25.93	10.80	19.49	35.61	0.00	24.62	11.19	0.00	28.77	10.39	9.26	26.50	10.99	27.63																			
openness of street profile	0.31	0.28	0.28	0.17	0.25	0.73	0.02	0.64	0.19	0.01	0.60	0.24	0.20	0.46	0.27	0.53																			
width deviation of street profile	4.24	2.82	3.27	1.90	2.61	0.70	0.01	5.40	2.12	0.00	4.27	3.76	1.84	3.14	1.35	2.49																			
linearity of street segment	0.95	0.99	1.00	1.00	1.00	0.88	1.00	0.83	1.00	1.00	0.94	1.00	0.99	0.99	1.00	0.99																			
area covered by edge-attached ETCs	17318.29	12742.99	12991.35	5746.13	11451.29	949462.29	675071.11	606875.99	7348.92	500189.57	58964.51	44804.08	7562.67	28095.50	6588.36	344638.99																			
buildings per meter of street segment	0.17	0.13	0.12	0.19	0.13	0.07	0.26	0.09	0.21	0.29	0.08	0.21	0.18	0.08	0.09	0.05																			
cells reached within neighbouring street segments	59.89	40.30	77.17	56.42	50.30	31.35	104.87	40.68	58.46	128.00	26.71	142.54	31.04	30.57	28.04	33.97																			
reached area by neighbouring segments	32945.34	24130.47	55557.33	18650.79	31303.76	1096925.49	39320.29	285174.65	157479.46	500189.57	75103.41	122982.39	11400.98	51087.36	7055.08	244919.70																			
mean segment length within 3 steps	2935.57	2800.72	5709.31	2662.70	3853.49	1057.56	892.18	3485.36	250148	441.35	3362.06	6775.42	1636.41	3870.56	1592.82	4880.63																			
node degree of junction	3.18	3.43	3.95	3.56	3.65	1.42	1.07	2.87	3.47	1.00	3.08	3.17	3.22	3.51	3.52	2.66																			
local meshness of street network	0.18	0.21	0.31	0.24	0.26	0.00	0.04	0.11	0.22	0.00	0.15	0.23	0.17	0.21	0.24	0.15																			
local proportion of 3-way intersections of street network	0.58	0.62	0.22	0.47	0.38	0.04	0.12	0.59	0.51	0.00	0.53	0.55	0.45	0.46	0.45	0.63																			
local proportion of 4-way intersections of street network	0.27	0.37	0.69	0.46	0.53	0.00	0.05	0.10	0.39	0.00	0.22	0.13	0.25	0.40	0.43	0.14																			
local proportion of cul-de-sacs of street network	0.05	0.04	0.01	0.02	0.03	0.71	0.74	0.14	0.03	1.00	0.09	0.04	0.04	0.05	0.06	0.18	0.04																		
local closeness of street network	0.00	0.00	0.00	0.00	0.00	0.00	0.00	0.00	0.00	0.00	0.00	0.00	0.00	0.00	0.00	0.00																			
local cul-de-sac length of street network	68.18	39.30	19.83																																

	0	1	2	3	4	5	6	7	8	9	10	11	12	13	14	15	16	17	18	
orientation of ETC	32.00	21.22	21.91	20.44	22.40	14.40	21.99	0.08	23.14	18.94	22.32	20.54	22.23	21.99	21.34	12.63	20.93	23.06	20.86	
orientation of building	32.56	21.03	21.23	19.79	20.77	13.67	21.74	0.00	0.00	18.69	19.94	19.45	20.14	22.39	20.78	11.81	20.86	23.43	19.65	
cell alignment of building	2.89	4.49	8.71	5.96	14.28	3.08	4.41	0.00	0.00	3.00	12.82	8.92	13.87	14.26	8.47	2.69	2.47	13.44	10.02	
longest axis length of ETC	29.06	31.96	27.33	19.39	187.90	35.41	31.03	0.04	1.52	18.76	95.69	70.50	116.55	384.46	21.50	26.73	52.02	151.06	60.84	
area of ETC	249.54	681.05	505.88	158.22	2079.24	460.31	447.06	0.00	0.00	139.88	475.34	2079.54	8259.09	80796.86	191.56	206.73	885.19	18840.75	3424.38	
circular compactness of ETC	0.36	0.41	0.46	0.44	0.39	0.39	0.38	0.23	0.07	0.43	0.40	0.45	0.42	0.31	0.40	0.35	0.37	0.40	0.42	
equivalent rectangular index of ETC	0.92	0.93	0.94	0.93	0.95	0.92	0.93	0.86	0.87	0.94	0.96	0.95	0.96	0.88	0.58	0.92	0.93	0.96	0.95	
covered area ratio of ETC	0.57	3.19	0.87	3.01	0.03	0.54	0.66	0.00	0.00	0.63	0.09	0.28	0.05	0.02	0.62	0.56	0.59	0.05	0.24	
alignment of neighbouring buildings	1.60	3.13	7.80	6.20	12.47	1.87	3.30	0.00	0.00	1.78	11.26	8.01	11.38	12.45	7.58	1.16	2.09	12.01	8.43	
mean distance between neighbouring buildings	2.64	9.08	8.69	3.47	98.74	3.91	5.35	0.00	0.00	2.29	45.92	21.85	56.91	215.57	5.28	2.62	5.02	79.46	25.87	
perimeter-weighted neighbours of ETC	0.07	0.12	0.12	0.13	0.03	0.06	0.09	41.11	26.26	0.12	0.04	0.04	0.05	0.31	0.13	0.08	0.05	0.03	0.08	
area covered by neighbouring cells	1652.72	6789.83	5027.92	1308.56	179569.31	3622.71	4189.46	289.87	269021.64	1038.89	45754.55	17898.55	71628.39	736784.74	2785.13	1438.21	7263.35	153862.36	29810.80	
mean inter-building distance	4.29	14.12	12.56	5.24	126.43	7.10	8.95	32.25	360.47	3.90	65.12	27.95	76.73	317.06	7.44	4.25	8.39	108.94	35.53	
street alignment of ETC	4.19	10.31	14.30	11.24	15.95	4.30	7.70	5.29	18.35	8.16	17.75	11.07	14.81	15.19	12.20	3.77	4.06	14.62	14.26	
weighted reached enclosures of ETC	0.00	0.00	0.00	0.00	0.00	0.00	0.00	0.00	0.00	0.00	0.00	0.00	0.00	0.00	0.00	0.00	0.00	0.00	0.00	
area of building	129.25	87.55	59.13	62.33	88.95	191.97	132.40	0.00	0.00	61.65	76.17	419.95	94.51	146.69	61.69	99.68	413.24	76.27	84.23	
perimeter of building	56.51	39.88	32.05	34.43	37.40	64.18	49.34	0.00	0.00	35.66	36.16	85.28	38.51	46.25	33.33	48.11	84.48	35.13	37.67	
courtyard area of building	1.36	1.20	0.13	0.15	0.04	2.22	1.42	0.00	0.00	0.19	0.07	5.39	0.18	0.21	0.15	0.44	3.60	0.16	0.46	
circular compactness of building	0.40	0.46	0.50	0.47	0.53	0.45	0.43	0.00	0.00	0.45	0.52	0.49	0.54	0.51	0.40	0.42	0.53	0.50	0.50	
corners of building	8.81	7.88	6.21	6.51	5.86	10.62	7.98	0.00	0.00	6.36	6.12	15.85	6.38	5.46	6.61	7.45	7.56	5.95	6.59	
squareness of building	4.75	3.37	6.27	7.91	2.11	4.52	5.19	0.00	0.00	3.02	3.30	10.33	2.93	0.75	5.89	3.82	7.46	1.97	4.66	
equivalent rectangular index of building	0.88	0.92	0.94	0.94	0.96	0.87	0.91	0.00	0.00	0.92	0.95	0.89	0.95	0.97	0.95	0.91	0.93	0.96	0.94	
elongation of building	0.45	0.57	0.65	0.61	0.68	0.53	0.51	0.00	0.00	0.54	0.69	0.64	0.71	0.64	0.65	0.45	0.49	0.68	0.65	
centroid - corner mean distance of building	7.84	5.76	5.02	5.33	6.00	8.51	7.09	0.00	0.00	5.61	5.62	10.40	5.96	7.87	5.02	7.15	13.09	5.56	5.79	
centroid - corner distance deviation of building	2.07	1.05	0.76	0.93	0.75	2.07	1.48	0.00	0.00	0.95	0.84	2.41	0.76	0.81	0.80	1.65	1.95	0.75	0.90	
shared walls ratio of buildings	0.52	0.48	0.30	0.49	0.02	0.46	0.48	0.00	0.00	0.64	0.05	0.08	0.02	0.00	0.00	1.15	0.54	0.57	0.03	0.17
perimeter wall length of adjacent buildings	418.21	193.58	97.49	251.70	39.24	384.81	358.45	0.00	0.00	236.70	43.61	101.24	39.87	46.91	86.19	435.97	426.63	50.59	79.63	
street alignment of building	3.43	9.85	10.21	11.13	15.54	3.87	7.51	0.00	0.00	5.46	15.82	11.03	14.34	16.30	11.64	2.76	4.04	14.13	13.65	
number of courtyards within adjacent buildings	25.85	5.92	0.66	4.02	0.00	21.93	12.83	0.00	0.00	9.78	0.03	0.24	0.01	0.00	0.42	24.93	7.34	0.07	0.81	
length of street segment	102.16	206.88	345.99	136.02	2294.91	113.61	119.07	147.95	166.49	86.58	11.41	182.46	574.45	2218.53	329.08	110.69	146.30	8627.78	650.55	
width of street profile	16.01	23.20	15.23	12.20	26.67	21.08	17.44	21.82	26.43	12.59	0.00	28.57	26.86	30.54	13.41	16.03	22.84	24.95	19.06	
openness of street profile	0.20	0.44	0.27	0.13	0.88	0.26	0.25	0.62	0.64	0.21	0.00	0.54	0.82	0.93	0.24	0.20	0.35	0.91	0.55	
width deviation of street profile	2.81	4.28	5.45	4.33	4.72	2.90	3.57	5.39	4.74	3.41	0.00	4.16	5.19	5.21	5.44	2.45	2.93	6.33	5.26	
linearity of street segment	0.99	0.90	0.82	0.92	0.78	0.98	0.95	0.98	0.84	0.97	1.00	0.87	0.84	0.80	0.83	0.99	0.98	0.65	0.82	
area covered by edge-attached ETCs	6574.92	37019.65	86677.28	12422.68	427374.41	9680.34	12112.06	62174.04	4764663.41	5095.78	1956088.80	28087.85	716827.90	1753477.48	63319.75	7058.48	15790.61	13818376.42	515392.82	
buildings per meter of street segment	0.22	0.50	0.79	0.55	0.40	0.16	0.28	0.10	0.76	0.34	27.83	0.08	0.47	0.82	0.79	0.28	0.12	0.10	0.57	
cells reached within neighbouring street segments	92.79	207.15	417.52	193.42	375.25	50.30	89.96	291.00	186.44	81.50	63.40	23.32	174.57	331.15	506.59	127.87	48.78	793.40	358.12	
reached area by neighbouring segments	25287.45	84039.85	176840.41	31791.92	6854414.53	18903.80	23754.86	11775.33	52757504.11	10939.75	4080464.96	42701.705	1300957.52	12663047.75	131564.46	23762.07	30176.93	1977293.48	103172.50	
mean segment length within 3 steps	3011.19	2282.12	2731.38	1922.60	7583.32	2432.24	1965.50	6736.40	2620.25	1616.82	33.06	1956.55	4021.53	5966.11	2640.92	3197.15	3389.34	16313.39	4435.94	
node degree of junction	3.63	2.52	2.41	2.71	1.91	3.34	2.97	3.00	1.22	3.20	1.00	2.66	1.84	1.26	1.28	3.63	3.48	2.59	2.32	
local meshedness of street network	0.24	0.08	0.08	0.13	0.05	0.20	0.14	0.11	0.02	0.18	0.00	0.09	0.02	0.05	0.09	0.23	0.21	0.07	0.05	
local proportion of 3-way intersections of street network	0.50	0.64	0.64	0.66	0.44	0.65	0.66	0.72	0.40	0.70	0.26	0.72	0.45	0.31	0.71	0.44	0.54	0.53	0.61	
local proportion of 4-way intersections of street network	0.46	0.11	0.08	0.18	0.02	0.30	0.21	0.10	0.02	0.23	0.00	0.09	0.01	0.01	0.07	0.50	0.40	0.01	0.04	
local proportion of cul-de-sacs of street network	0.03	0.24	0.27	0.15	0.44	0.03	0.11	0.18	0.58	0.07	0.76	0.18	0.52	0.64	0.22	0.05	0.03	0.32	0.34	
local closeness of street network	0.00	0.00	0.00	0.00	0.00	0.00	0.00	0.00	0.00	0.00	0.00	0.00	0.00	0.00	0.00	0.00	0.00	0.00	0.00	
local cul-de-sac length of street network	23.96	287.62	389.55	163.46	1333.91	26.89	139.24	0.00	441.63	59.98	33.06	241.77	805.43	1490.58	408.42	62.76	38.06	2435.34	987.30	
square clustering of street network	0.07	0.02	0.03	0.04	0.01	0.07	0.05	0.10	0.10	0.01	0.07	0.00	0.02	0.01	0.01	0.01	0.07	0.05	0.02	
mean distance to neighbouring nodes of street network	84.64	150.27	235.01	105.13	1245.02	85.43	90.97	152.56	167.00	62.80	11.41	134.96	408.79	1604.09	218.69	88.94	106.61	4201.23	421.87	
local node density of street network	0.01	0.02	0.01	0.02	0.00	0.02	0.02	0.01	0.01	0.02	0.00	0.02	0.01	0.00	0.01	0.01	0.01	0.00	0.01	
local degree weighted node density of street network	0.03	0.03	0.02	0.04	0.00	0.03	0.04	0.01	0.01	0.04	0.00	0.03	0.01	0.00	0.02	0.03	0.03	0.00	0.01	
area covered by node-attached ETCs	6729.83	24726.08	59141.25	10373.80	2516477.73	6165.48	7606.40	13491.51	3828032.62	3417.89	1954758.04	16065.44	514041.77	45360.67	7122896.26	4377.05	990.91	7482893.35	314998.25	
perimeter of enclosure	439.93	5024.44	5749.57	2229.99	4193.04	514.22	1216.59	0.10	3.04	572.74	2775.00	3713.25	433867.60	47396.08	3309.13	467.46	631.87	38277.65	39230.94	
circular compactness of enclosure	0.48	0.37	0.31	0.35	0.39	0.42	0.41	0.23	0.07	0.39	0.44	0.41	0.39	0.36	0.30	0.48	0.46	0.35	0.39	
equivalent rectangular index of enclosure	0.97	0.70	0.63	0.73	0.63	0.95	0.86	0.86	0.87	0.93	0.67	0.76	0.76	0.51	0.58	0.73	0.97	0.96	0.71	0.57
compactness-weighted axis of enclosure	75.38</td																			

	0	1	2	3	4	5	6	7	8	9	10	11	12	13	14	15
area of building	84.68	78.34	124.22	93.07	70.02	109.53	106.00	273.28	101.88	222.98	95.73	69.58	79.42	112.55	97.48	144.20
perimeter of building	36.03	35.09	43.74	38.67	33.53	42.01	42.03	57.67	40.03	54.46	38.77	32.99	36.32	42.40	38.49	52.77
courtyard area of building	0.02	0.08	0.07	0.03	0.05	0.04	0.08	0.00	0.04	0.89	0.02	0.04	0.06	0.03	0.04	0.00
circular compactness of building	0.55	0.53	0.56	0.55	0.53	0.55	0.51	0.55	0.55	0.50	0.55	0.53	0.52	0.53	0.56	0.62
corners of building	4.87	5.93	5.37	4.82	5.66	5.03	6.91	5.40	4.99	5.93	4.99	5.67	5.87	5.56	4.93	12.69
squareness of building	1.37	1.07	0.77	0.52	0.91	0.47	1.20	3.18	0.59	1.85	0.59	1.13	1.37	0.98	0.62	0.37
equivalent rectangular index of building	0.98	0.96	0.97	0.98	0.96	0.97	0.94	0.96	0.98	0.96	0.98	0.96	0.95	0.96	0.98	0.91
elongation of building	0.68	0.67	0.71	0.68	0.68	0.69	0.66	0.71	0.70	0.61	0.69	0.68	0.67	0.67	0.70	0.79
centroid - corner mean distance of building	6.15	5.82	7.23	6.58	5.44	7.05	6.46	8.94	6.74	8.95	6.54	5.35	5.80	6.88	6.51	6.96
centroid - corner distance deviation of building	0.39	0.69	0.56	0.44	0.59	0.53	0.97	0.81	0.46	0.93	0.45	0.60	0.72	0.74	0.41	1.21
orientation of building	19.78	18.83	17.10	16.97	18.08	13.07	19.63	13.74	18.77	19.97	18.37	19.58	17.46	34.05	17.15	27.88
longest axis length of ETC	48.46	20.95	75.60	28.41	19.32	32.86	23.58	365.43	46.17	52.92	40.81	18.89	32.55	57.99	41.41	
area of ETC	4458.60	2176.5	2995.35	384.67	183.00	4872.22	259.82	71961.99	1002.27	2127.36	851.98	173.97	159.35	502.92	2058.59	672.32
circular compactness of ETC	0.48	0.51	0.45	0.52	0.52	0.50	0.50	0.40	0.47	0.46	0.49	0.52	0.53	0.49	0.47	0.48
equivalent rectangular index of ETC	0.97	0.96	0.96	0.98	0.97	0.97	0.96	0.91	0.97	0.96	0.98	0.97	0.97	0.97	0.97	0.97
orientation of ETC	21.78	20.38	20.82	19.84	19.78	17.38	20.56	19.75	21.46	21.48	21.39	20.94	18.39	29.75	20.95	27.28
covered area ratio of ETC	0.22	0.45	0.10	0.32	0.45	0.30	0.52	0.02	0.17	0.24	0.20	0.45	0.51	0.30	0.15	0.22
cell alignment of building	12.15	7.81	13.02	10.07	7.64	9.73	5.74	10.59	12.45	9.68	12.59	8.04	6.71	8.58	13.45	2.97
alignment of neighbouring buildings	8.69	6.16	9.15	7.65	6.25	6.66	5.35	6.83	9.13	6.42	9.37	6.70	5.87	4.83	9.48	2.64
mean distance between neighbouring buildings	14.45	4.65	36.13	8.47	4.14	10.05	4.15	266.42	18.57	19.22	15.93	4.07	3.24	9.32	26.10	13.71
perimeter-weighted neighbour of building	0.07	0.12	0.04	0.09	0.13	0.07	0.10	0.01	0.00	0.06	0.07	0.13	0.13	0.08	0.05	0.05
area covered by neighbouring cells	100067.95	1752.91	41352.05	3003.80	1473.52	3577.06	1871.58	2171413.77	8360.73	58490.06	6981.14	1429.47	1246.24	3710.29	23925.08	4330.68
weighted reached enclosure of ETC	0.00	0.00	0.00	0.00	0.00	0.00	0.00	0.00	0.00	0.00	0.00	0.00	0.00	0.00	0.00	0.00
mean inter-building distance	45.28	7.07	54.83	10.26	5.26	12.26	5.19	521.65	22.73	39.39	19.77	5.42	3.85	11.56	37.91	18.26
reached ETCs by tessellation contiguity	46.45	44.10	46.00	42.19	43.69	38.90	37.23	120.29	42.79	51.33	44.23	43.95	43.51	37.14	44.23	30.33
reached area by tessellation contiguity	985601.06	136875.2	415904.32	22376.23	10427.87	25347.26	1319.73	1691478.27	62823.59	596010.54	55752.48	10684.00	8424.71	26937.91	219986.77	27386.36
width of street profile	37.48	20.58	31.51	21.48	15.84	23.06	19.18	49.78	26.96	31.13	24.95	24.74	30.82	24.70	28.09	31.85
width deviation of street profile	3.16	4.53	3.99	5.33	4.83	4.99	4.17	0.03	4.86	4.07	5.24	4.41	6.41	4.81	4.55	2.58
openness of street profile	0.85	0.42	0.81	0.49	0.31	0.54	0.41	0.99	0.69	0.67	0.64	0.46	0.69	0.52	0.76	0.58
length of street segment	646.34	2016.3	190.14	196.00	244.34	140.89	178.23	166.92	175.98	311.31	216.17	498.20	2994.60	181.82	204.77	158.17
linearity of street segment	0.94	0.94	0.93	0.93	0.90	0.90	0.96	0.94	0.94	0.94	0.90	0.94	0.88	0.96	0.92	0.96
mean segment length within 3 steps	3911.78	2313.43	2152.28	2038.15	1472.84	2111.95	2349.10	2628.85	2283.82	3248.45	1336.63	3911.97	8934.05	2547.94	1635.47	1636.31
node degree of junction	2.92	2.83	2.67	2.68	2.02	2.96	3.11	3.04	2.83	2.89	2.13	2.88	3.56	3.00	2.41	2.83
local meshedness of street network	0.10	0.11	0.09	0.08	0.04	0.12	0.16	0.11	0.09	0.11	0.04	0.09	0.13	0.12	0.07	0.13
local proportion of 3-way intersections of street network	0.72	0.72	0.70	0.65	0.48	0.79	0.71	0.69	0.74	0.71	0.47	0.71	0.63	0.75	0.59	0.72
local proportion of 4-way intersections of street network	0.08	0.10	0.05	0.07	0.03	0.08	0.19	0.09	0.07	0.12	0.03	0.08	0.26	0.11	0.04	0.03
local proportion of cul-de-sacs of street network	0.19	0.18	0.24	0.27	0.48	0.12	0.10	0.19	0.19	0.16	0.50	0.21	0.11	0.14	0.35	0.25
local closeness of street network	0.00	0.00	0.00	0.00	0.00	0.00	0.00	0.00	0.00	0.00	0.00	0.00	0.00	0.00	0.00	0.00
local cul-de-sac length of street network	565.15	237.19	317.11	354.77	439.27	15.494	111.65	309.23	249.35	262.34	433.50	409.80	89.24	208.41	397.49	259.00
square clustering of street network	0.02	0.04	0.03	0.03	0.01	0.04	0.05	0.05	0.03	0.04	0.01	0.03	0.05	0.04	0.03	0.06
mean distance to neighbouring nodes of street network	362.07	140.70	151.71	147.64	213.83	105.68	112.02	157.09	133.57	194.73	178.61	280.26	922.71	130.23	163.06	114.81
local node density of street network	0.01	0.02	0.01	0.02	0.01	0.02	0.02	0.01	0.02	0.01	0.01	0.01	0.01	0.01	0.02	0.01
local degree weighted node density of street network	0.02	0.03	0.02	0.02	0.01	0.03	0.03	0.02	0.03	0.02	0.02	0.02	0.02	0.03	0.02	0.02
area of enclosure	13343053.23	1187723.49	11803942.15	7150735.02	2535723.25	766008.79	150022.88	5872625.61	2603732.27	3164305.56	1423819.15	2381879.17	1681849.54	536338.11	6779807.16	10570617.89
perimeter of enclosure	53847.89	7122.74	50813.28	31755.96	12875.33	4160.48	1559.83	24428.02	12359.67	17703.76	55596.77	111618.02	10424.33	3676.13	26393.05	31172.30
circular compactness of enclosure	0.31	0.38	0.36	0.36	0.37	0.44	0.42	0.39	0.40	0.36	0.35	0.37	0.33	0.41	0.13	0.43
equivalent rectangular index of enclosure	0.57	0.69	0.57	0.50	0.57	0.86	0.90	0.85	0.73	0.75	0.36	0.62	0.61	0.85	0.20	0.65
compactness-weighted axis of enclosure	8261.22	1574.62	8536.11	5148.82	2630.77	682.18	366.06	4645.73	2138.71	3987.60	8465.67	2434.07	2462.25	804.64	37597.45	4329.96
orientation of enclosure	23.51	21.64	21.94	21.35	21.67	15.88	20.69	20.53	21.22	22.76	21.79	27.16	18.85	32.26	30.88	15.96
perimeter-weighted neighbour of enclosure	0.01	0.01	0.01	0.00	0.00	0.01	0.01	0.01	0.01	0.01	0.05	0.00	0.01	0.01	0.00	0.01
area-weighted ETCs of enclosure	0.00	0.01	0.00	0.00	0.01	0.00	0.01	0.01	0.00	0.06	0.56	0.00	0.01	0.00	0.00	0.00
street alignment of building	14.52	13.82	12.84	14.22	14.85	11.61	8.89	7.42	13.61	12.02	15.06	14.27	10.07	9.99	14.25	6.30
area covered by node-attached ETCs	268160.96	277216.2	33470.10	30920.48	48143.50	15000.44	16360.61	91280.03	23538.25	48521.88	41550.56	116375.18	360881.76	19383.03	46882.26	11118.93
area covered by edge-attached ETCs	682511.88	322227.9	51098.55	35505.99	53036.46	19094.90	1871.87	1305194.03	31522.16	78710.70	51691.07	129864.59	388560.55	26185.77	660172.22	15843.16
buildings per meter of street segment	0.26	0.77	0.12	0.47	1.87	0.24	0.36	0.01	0.18	0.23	0.40	1.56	0.70	0.26	0.29	0.11
reached ETCs by neighbouring segments	256.31	283.02	45.62	185.00	480.89	85.70	150.48	5.64	73.67	134.65	125.52	105.31	2217.54	115.57	85.07	37.40
reached area by neighbouring segments	1865873.94	78888.67	152221.82	88524.89	94595.65	58529.83	47345.22	624221.29	98907.43	234290.59	102045.27	255266.27	468612.06	80734.10	141823.95	45919.25
reached ETCs by local street network	568.37	904.10	139.67	541.41	998.99	327.13	521.55	13.10	249.70	452.90	255.34	2469.86	2683.83	435.64	196.68	119.18
reached area by local street network	5152225.43	290465.98	547579.54	289902.41	221249.58	250118.26	198643.56	2613433.19	376470.48	823127.62	240815.53	727864.75	978914.95	346410.67	391381.53	176852.67
population	44.95	287.54	16.61	147.78	368.44	102.81	259.58	16.90	35.94	92.53	57.38	321.73	470.30	125.00	19.59	5.81
night lights	7.03	17.35	6.24	11.19	15.50	10.65	22.39	3.02	8.10	24.33	8.73	15.71	21.70	16.37	5.06	5.94
NDVI	0.32	0.12	0.45	0.23	0.11	0.24	0.11	0.47	0.38	0.26	0.37	0.11	0.07	0.22	0.40	0.25

	0	1	2	3	4	5	6	7	8	9
area of building	327.72	293.21	326.46	308.53	313.96	259.92	327.04	268.65	267.60	337.34
perimeter of building	70.00	67.02	69.38	68.62	68.21	63.44	70.29	64.71	65.09	70.70
courtyard area of building	0.00	0.00	0.00	0.00	0.00	0.00	0.00	0.00	0.00	0.00
circular compactness of building	0.55	0.54	0.54	0.54	0.54	0.54	0.54	0.54	0.54	0.54
corners of building	5.15	5.07	5.15	5.16	5.13	5.03	5.15	5.04	5.04	5.17
squareness of building	0.33	0.30	0.34	0.28	0.35	0.31	0.32	0.28	0.29	0.32
equivalent rectangular index of building	0.96	0.96	0.96	0.96	0.96	0.97	0.96	0.96	0.96	0.96
elongation of building	0.73	0.72	0.72	0.73	0.71	0.71	0.72	0.71	0.71	0.72
centroid - corner mean distance of building	11.37	10.98	11.28	11.10	11.12	10.44	11.42	10.62	10.71	11.46
centroid - corner distance deviation of building	1.19	1.12	1.22	1.21	1.16	1.04	1.21	1.08	1.09	1.24
orientation of building	14.12	12.91	12.95	12.09	14.31	10.69	12.87	12.02	14.63	12.79
longest axis length of ETC	97.51	94.90	97.46	95.75	100.82	90.82	100.05	108.64	115.34	92.55
area of ETC	7410.02	7084.84	6260.85	8496.11	7777.43	5940.12	7574.58	10203.40	11301.86	6416.87
circular compactness of ETC	0.43	0.43	0.43	0.44	0.43	0.43	0.43	0.44	0.44	0.43
equivalent rectangular index of ETC	0.95	0.95	0.95	0.95	0.00	0.95	0.00	0.95	0.95	0.95
orientation of ETC	16.78	15.86	16.04	15.15	17.19	14.16	15.74	15.50	17.41	15.51
covered area ratio of ETC	0.21	0.19	1844961.01	0.21	1709654232401.38	0.25	0.20	0.17	0.17	0.22
cell alignment of building	7.09	6.80	7.14	6.70	7.19	6.43	7.10	7.26	7.27	6.69
alignment of neighbouring buildings	5.73	4.98	5.35	5.12	5.42	3.95	5.56	4.86	5.51	5.20
mean distance between neighbouring buildings	37.76	37.19	37.47	37.08	39.94	36.43	39.58	46.67	49.42	34.49
perimeter-weighted neighbours of ETC	0.03	0.03	9675.98	0.03	10388.16	0.03	5053.99	0.03	1337.49	0.03
area covered by neighbouring cells	73124.21	70936.95	61823.75	82627.94	82077.66	51660.86	74325.94	92353.95	118286.69	60611.61
weighted reached enclosures of ETC	0.00	0.00	0.00	0.00	0.00	0.00	0.00	0.00	0.00	0.00
mean inter-building distance	55.70	55.91	55.90	54.41	62.86	51.00	56.83	66.60	74.33	51.37
reached ETCs by tessellation contiguity	42.25	39.61	41.89	40.02	41.88	37.07	42.33	38.83	39.79	42.39
reached area by tessellation contiguity	807002.53	802280.51	643197.79	914728.30	962109.13	466853.27	753704.29	916844.43	1078442.11	645525.13
width of street profile	37.29	36.42	37.17	36.94	37.19	35.73	37.50	36.84	37.56	37.07
width deviation of street profile	2.01	2.16	2.04	2.00	2.09	2.28	1.94	2.07	1.95	2.00
openness of street profile	0.64	0.63	0.65	0.61	0.65	0.62	0.65	0.66	0.66	0.63
length of street segment	240.64	244.35	245.73	241.14	239.72	265.02	243.42	253.26	256.91	232.44
linearity of street segment	0.89	0.90	0.89	0.90	0.89	0.91	0.89	0.91	0.89	0.89
mean segment length within 3 steps	2869.86	3093.53	2995.14	3088.03	2915.17	3456.52	2918.93	3280.17	3218.22	2918.36
node degree of junction	3.04	3.10	3.08	3.08	3.04	3.16	3.05	3.09	3.09	3.08
local meshedness of street network	0.13	0.14	0.14	0.13	0.13	0.15	0.13	0.13	0.13	0.14
local proportion of 3-way intersections of street network	0.64	0.62	0.64	0.63	0.63	0.61	0.64	0.62	0.63	0.64
local proportion of 4-way intersections of street network	0.19	0.22	0.20	0.21	0.20	0.24	0.19	0.21	0.20	0.21
local proportion of cul-de-sacs of street network	0.16	0.15	0.15	0.16	0.16	0.14	0.16	0.16	0.16	0.15
local closeness of street network	0.00	0.00	0.00	0.00	0.00	0.00	0.00	0.00	0.00	0.00
local cul-de-sac length of street network	236.57	224.32	224.52	237.98	239.35	200.53	236.36	246.84	251.53	212.86
square clustering of street network	0.05	0.05	0.05	0.05	0.05	0.06	0.05	0.05	0.06	0.05
mean distance to neighbouring nodes of street network	165.76	168.05	168.04	166.89	168.14	176.00	168.15	176.46	179.30	160.79
local node density of street network	0.01	0.01	0.01	0.01	0.01	0.01	0.01	0.01	0.01	0.01
local degree weighted node density of street network	0.03	0.03	0.03	0.03	0.03	0.02	0.03	0.02	0.02	0.03
area of enclosure	2088654.94	2099464.01	2403092.25	2321284.06	3025585.47	1493985.32	2096686.06	3271902.86	3511102.38	1751316.01
perimeter of enclosure	7915.18	7938.35	8778.50	6910.67	11164.93	5906.86	7228.77	10345.48	8447.24	6498.26
circular compactness of enclosure	0.38	0.39	0.38	0.39	0.38	0.38	0.39	0.39	0.39	0.38
equivalent rectangular index of enclosure	0.75	0.79	0.77	0.79	0.00	0.80	0.00	0.78	0.81	0.78
compactness-weighted axis of enclosure	1501.06	1490.23	1581.17	1349.15	1965.10	1191.13	1432.80	1913.97	1758.65	1251.33
orientation of enclosure	15.21	14.25	14.29	12.69	16.04	12.79	13.92	13.41	15.61	13.39
perimeter-weighted neighbours of enclosure	0.01	0.01	9675.94	0.01	10388.14	0.01	5053.97	0.01	1337.47	0.01
area-weighted ETCs of enclosure	12917.17	3694.24	13967786396130.80	0.00	17286013846484.13	14965.23	6983978563793.46	7092.00	683701978481.85	14778.06
street alignment of building	9.01	7.99	8.34	8.43	8.39	6.62	8.90	7.49	8.24	8.50
area covered by edge-attached ETCs	83146.71	80788.40	75418.22	89686.73	92256.54	67653.86	80919.20	97932.93	126249.03	71867.00
buildings per meter of street segment	0.07	0.07	0.07	0.08	0.07	0.08	0.07	0.07	0.07	0.07
reached ETCs by neighbouring segments	41.37	42.79	41.08	44.69	40.37	46.51	40.92	41.80	40.63	41.80
reached area by neighbouring segments	281488.88	272526.09	254712.59	310589.04	304537.46	224088.61	277892.15	328342.31	381866.46	244265.91
reached ETCs by local street network	139.12	150.53	142.67	159.72	134.57	174.45	140.43	153.10	148.17	144.99
reached area by local street network	1092958.69	1074387.88	988337.66	1238410.28	1172441.88	919602.63	1063399.76	1260479.66	1399168.47	979008.15
area covered by node-attached ETCs	32871.34	31903.15	34456.37	29772.13	33129.92	28516.60	34612.87	36598.10	39750.77	29809.64
Workplace population - class CNS01	0.00	0.00	0.00	0.00	0.00	0.00	0.00	0.01	0.01	0.00
Workplace population - class CNS02	0.01	0.05	0.00	0.01	0.37	0.00	0.00	0.02	0.01	0.00
Workplace population - class CNS03	0.00	0.01	0.00	0.00	0.08	0.00	0.00	0.00	0.00	0.01
Workplace population - class CNS04	0.10	0.20	0.03	0.03	0.51	0.02	0.02	0.10	0.08	0.04
Workplace population - class CNS05	0.09	0.23	0.02	0.03	0.51	0.00	0.00	0.10	0.08	0.04
Workplace population - class CNS06	0.07	0.11	0.02	0.02	0.56	0.01	0.01	0.03	0.02	0.03
Workplace population - class CNS07	0.12	0.11	0.06	0.06	1.08	0.01	0.01	0.03	0.01	0.06
Workplace population - class CNS08	0.04	0.13	0.01	0.03	0.43	0.03	0.01	0.03	0.04	0.01
Workplace population - class CNS09	0.01	0.01	0.00	0.01	0.15	0.00	0.00	0.00	0.00	0.00
Workplace population - class CNS10	0.03	0.02	0.02	0.03	0.42	0.00	0.00	0.00	0.00	0.01
Workplace population - class CNS11	0.02	0.02	0.01	0.02	0.22	0.00	0.00	0.01	0.01	0.01
Workplace population - class CNS12	0.06	0.05	0.03	0.03	0.96	0.01	0.01	0.02	0.01	0.03
Workplace population - class CNS13	0.01	0.01	0.00	0.00	0.24	0.00	0.00	0.00	0.01	0.00
Workplace population - class CNS14	0.08	0.07	0.02	0.03	0.81	0.01	0.01	0.03	0.01	0.04
Workplace population - class CNS15	0.08	0.13	0.06	0.13	0.91	0.01	0.06	0.03	0.01	0.09
Workplace population - class CNS16	0.11	0.08	0.06	0.06	1.47	0.01	0.01	0.02	0.01	0.06
Workplace population - class CNS17	0.01	0.01	0.01	0.01	0.12	0.00	0.00	0.00	0.01	0.01
Workplace population - class CNS18	0.11	0.08	0.05	0.08	1.00	0.01	0.01	0.02	0.01	0.06

	0	1	2	3	4	5	6	7	8	9	10	11
orientation of ETC	21.27	25.40	18.51	20.99	29.10	23.38	19.53	22.22	22.54	20.64	20.55	22.89
orientation of building	21.04	23.62	18.26	20.54	29.07	22.49	29.31	21.50	21.23	19.38	18.58	23.10
cell alignment of building	3.94	8.48	1.57	5.88	1.81	5.45	19.80	7.23	7.21	7.37	6.98	12.65
longest axis length of ETC	68.88	239.53	41.49	172.83	50.80	74.44	355.27	77.85	63.23	142.19	111.48	391.24
area of ETC	2145.80	26027.87	430.60	13970.19	1032.20	3440.12	96663.37	3235.26	726.77	9561.04	4255.78	123271.66
circular compactness of ETC	0.39	0.40	0.31	0.40	0.29	0.39	0.56	0.46	0.23	0.38	0.40	0.33
equivalent rectangular index of ETC	0.95	0.00	0.96	0.92	0.94	0.00	0.86	0.00	0.90	0.00	0.00	0.00
covered area ratio of ETC	0.42	0.24	0.45	0.34	0.72	0.35	0.53	0.32	492.76	0.72	0.74	0.07
alignment of neighbouring buildings	3.54	6.34	1.87	3.26	1.85	4.75	13.70	6.90	0.04	6.37	7.39	9.09
mean distance between neighbouring buildings	15.52	112.29	7.20	56.98	8.23	21.68	158.24	22.83	1.79	45.64	25.32	201.05
perimeter-weighted neighbours of ETC	0.04	0.02	0.05	0.02	0.05	0.05	0.00	0.05	0.08	0.04	0.04	0.03
area covered by neighbouring cells	19184.11	357572.56	3591.07	179958.36	9640.09	37989.61	4143194.15	31796.08	14947.46	106708.01	41958.02	911032.66
mean inter-building distance	22.59	245.23	11.33	89.83	14.30	45.80	84.36	32.38	12.91	66.29	34.93	257.22
street alignment of ETC	6.81	7.57	5.46	9.89	4.29	9.33	20.11	10.46	4.99	8.96	9.01	16.27
weighted reached enclosures of ETC	0.00	0.00	0.00	0.00	0.00	0.00	0.00	0.00	0.00	0.00	0.00	0.00
area of building	480.85	1564.19	162.32	2145.16	398.56	350.28	607.25	480.34	14498.84	1782.96	1509.61	399.14
perimeter of building	90.65	129.89	55.75	176.88	77.15	73.31	307.72	90.43	758.82	195.71	231.86	85.98
courtyard area of building	6.22	5.74	0.11	9.45	1.52	0.00	0.00	4.89	0.00	21.48	30.66	3.58
circular compactness of building	0.47	0.63	0.43	0.48	0.35	0.48	0.59	0.52	0.32	0.43	0.38	0.48
corners of building	6.89	8.56	4.54	6.08	5.16	5.48	9.00	7.44	16.57	13.44	25.46	5.02
squareness of building	1.97	19.58	0.60	2.76	4.09	2.33	10.85	3.18	10.31	6.44	7.28	3.30
equivalent rectangular index of building	0.96	1.01	0.99	0.96	0.98	0.98	0.94	0.95	0.79	0.87	0.75	0.97
elongation of building	0.54	0.70	0.43	0.56	0.35	0.57	0.83	0.67	0.34	0.56	0.56	0.57
centroid - corner mean distance of building	14.32	21.88	10.38	29.14	13.91	12.97	46.57	13.62	99.38	26.36	25.95	14.89
centroid - corner distance deviation of building	1.45	1.30	0.36	2.79	0.93	0.75	3.97	1.79	17.80	4.86	6.61	1.20
shared walls ratio of buildings	0.24	0.03	0.45	0.11	0.61	0.22	-0.00	0.09	32.02	0.17	0.20	0.01
perimeter wall length of adjacent buildings	136.43	135.71	134.21	215.39	236.46	128.95	307.77	107.41	2274.26	325.16	315.08	88.23
street alignment of building	6.99	10.37	5.44	9.64	4.43	9.02	4.76	10.76	7.53	10.90	11.61	17.67
number of courtyards within adjacent buildings	0.03	0.01	0.00	0.03	0.03	0.01	0.00	0.02	0.03	0.25	0.24	0.01
length of street segment	149.39	274.05	207.12	225.83	114.93	201.86	2271.86	188.73	91.71	214.22	158.32	733.48
width of street profile	28.33	43.99	24.73	32.15	20.40	26.48	35.33	29.44	4.52	36.59	35.18	39.72
openness of street profile	0.45	0.90	0.28	0.65	0.33	0.48	0.93	0.50	0.12	0.71	0.63	0.94
width deviation of street profile	3.38	1.13	3.18	2.87	3.14	3.54	1.47	3.82	0.94	2.50	2.89	2.04
linearity of street segment	0.91	0.87	0.94	0.82	0.94	0.87	0.97	0.88	0.94	0.84	0.85	0.80
area covered by edge-attached ETCs	22867.13	291633.97	20900.40	101889.55	12488.32	96068.28	9666638.51	36085.42	17810.73	78759.77	35166.75	1906499.38
buildings per meter of street segment	0.10	0.02	0.18	0.04	0.17	0.15	0.02	0.08	0.14	0.03	0.03	0.12
cells reached within neighbouring street segments	26.32	4.64	78.95	6.74	32.87	40.43	24.00	23.57	3.15	6.33	5.71	65.57
reached area by neighbouring segments	27913.14	140766.90	39604.67	99885.47	14618.18	126126.15	10082656.72	44248.58	4098.31	56341.05	28081.45	3124591.48
mean segment length within 3 steps	1727.00	2799.43	2334.80	1566.97	1695.80	1477.94	5090.65	1736.70	973.08	2256.55	1657.84	3752.11
node degree of junction	2.83	3.05	3.05	2.59	3.15	2.39	1.50	2.62	3.39	2.97	2.99	2.17
local meshedness of street network	0.12	0.17	0.14	0.08	0.15	0.10	0.03	0.08	0.23	0.14	0.14	0.05
local proportion of 3-way intersections of street network	0.68	0.79	0.73	0.61	0.68	0.65	0.61	0.70	0.78	0.72	0.68	0.55
local proportion of 4-way intersections of street network	0.16	0.11	0.14	0.07	0.22	0.07	0.01	0.07	0.19	0.16	0.20	0.02
local proportion of cul-de-sacs of street network	0.16	0.10	0.13	0.32	0.10	0.28	0.38	0.22	0.01	0.12	0.11	0.43
local closeness of street network	0.00	0.00	0.00	0.00	0.00	0.00	0.00	0.00	0.00	0.00	0.00	0.00
local cul-de-sac length of street network	156.26	162.51	123.12	209.07	79.27	267.84	2566.33	207.43	17.98	114.20	98.78	1396.38
square clustering of street network	0.04	0.07	0.08	0.05	0.04	0.04	0.00	0.03	0.10	0.05	0.04	0.00
mean distance to neighbouring nodes of street network	105.42	182.00	134.58	150.91	77.14	144.58	2277.74	132.15	60.51	145.11	102.57	570.77
local node density of street network	0.02	0.01	0.01	0.02	0.03	0.02	0.00	0.02	0.04	0.02	0.02	0.01
local degree weighted node density of street network	0.04	0.02	0.03	0.03	0.05	0.03	0.00	0.03	0.09	0.04	0.05	0.01
area covered by node-attached ETCs	10531.12	79147.11	13484.25	43173.81	5441.54	63527.00	348309.27	17043.03	1528.14	24764.01	13371.28	1228990.58
area of enclosure	364105.97	941960.40	427492.03	299251.78	22607.13	19112399.67	11301559.65	928506.34	2135.90	448047.37	100796.64	9481343.06
perimeter of enclosure	3435.93	10618.89	3457.03	19213.02	644.13	101558.22	19627.23	7436.58	232.98	3765.68	1536.73	31973.79
circular compactness of enclosure	0.37	0.38	0.33	0.34	0.39	0.26	0.37	0.37	0.22	0.34	0.37	0.30
equivalent rectangular index of enclosure	0.75	0.00	0.83	0.61	0.90	0.00	0.68	0.00	0.88	0.00	0.00	0.00
compactness-weighted axis of enclosure	664.40	1256.18	603.18	2801.09	147.56	10926.76	3807.07	1212.61	94.14	750.79	373.64	4726.30
orientation of enclosure	21.65	24.89	19.45	20.82	29.05	25.54	36.37	22.06	22.56	21.29	21.21	20.11
perimeter-weighted neighbours of enclosure	0.01	0.02	0.01	0.01	0.02	0.00	0.00	0.02	0.08	0.03	0.03	0.03
area-weighted ETCs of enclosure	0.02	60657750.20	0.59	7556335.95	4025358.73	10111302.23	0.00	70596540.89	0.01	507875.35	6327673.47	1217322747.09
parks	319.49	6307.74	222.94	3541.05	315.85	1776.91	35268.04	671.64	3349.30	816.66	902.37	2532.90
easting establishments	157.50	2.64	91.51	15.54	1129.56	36.90	0.00	70.12	3.83	152.13	216.81	1.26
supermarkets	2.55	0.03	1.62	0.27	8.56	0.71	0.00	1.63	0.02	2.30	4.18	0.01
monuments	0.18	0.00	0.10	0.00	7.20	0.00	0.00	0.09	0.00	0.18	0.03	0.00
population	125.81	0.62	135.02	20.78	84.44	35.89	0.00	48.93	69.09	101.11	202.98	0.00
NDVI	0.19	0.09	0.16	0.19	0.09	0.25	0.03	0.29	-0.03	0.23	0.20	0.42
night lights	63.98	118.63	56.07	53.97	107.28	29.37	1.55	41.70	60.47	68.01	72.27	4.55

Figure 15: Mean values of characters per each cluster of the Singapore case study. Colour coding is row-normalised with blue colour indicating smaller while red indicating higher values. For details on the measurements, see the accompanying Jupyter notebook.

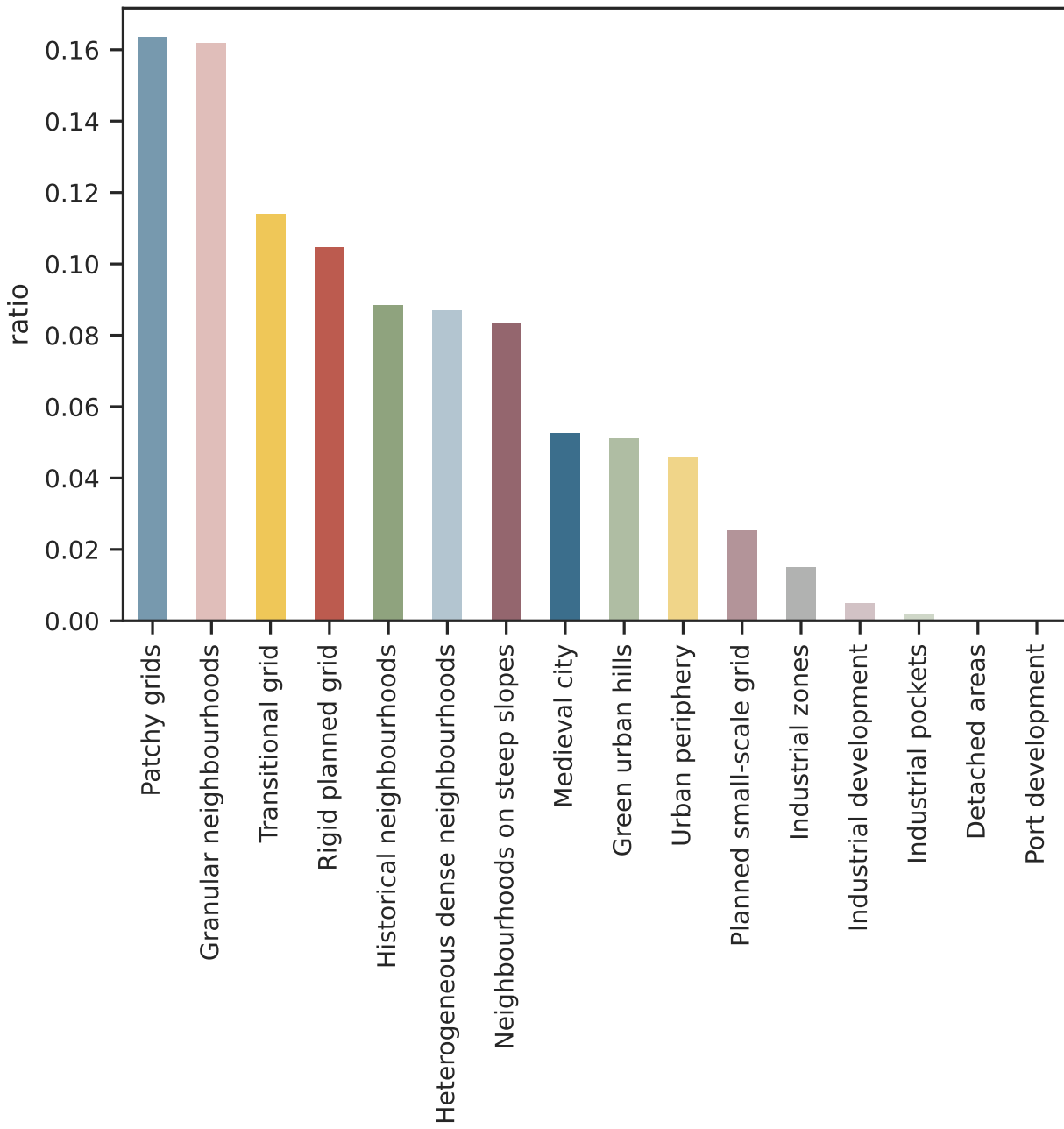


Figure 16: Proportion of enclosed tessellation cells belonging to the individual clusters of the Barcelona case study.

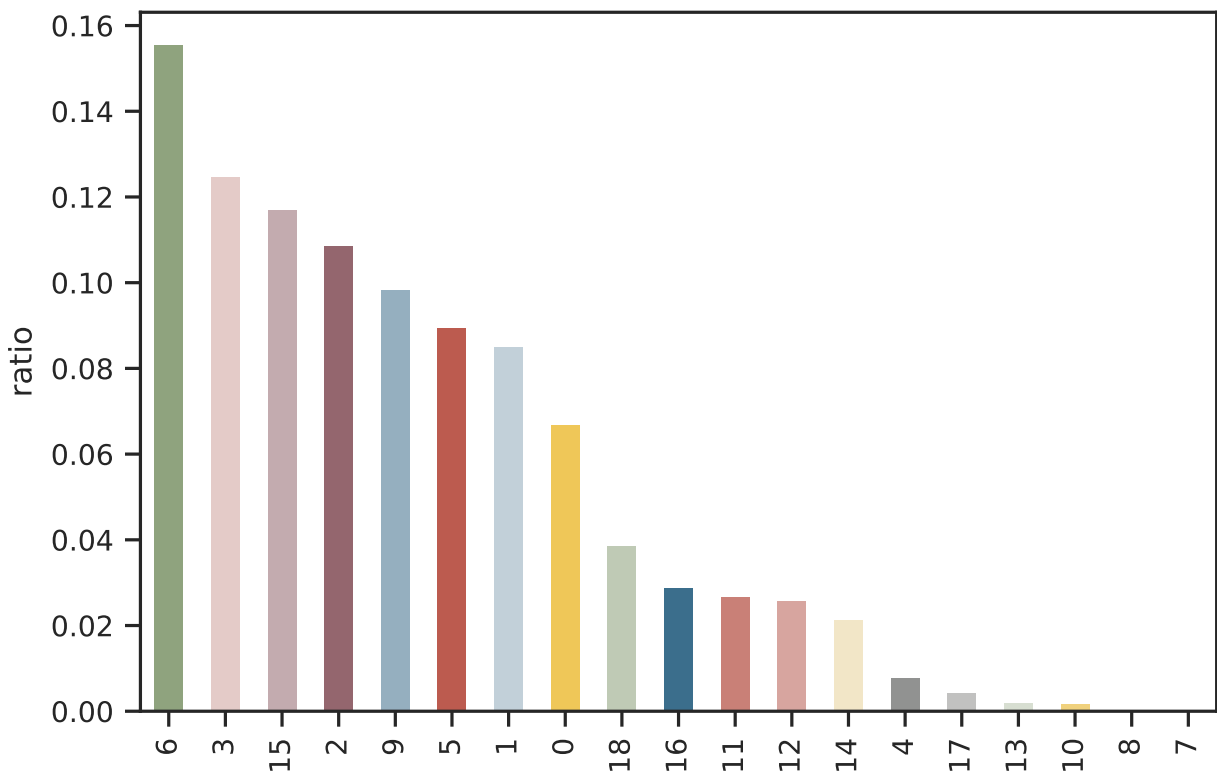


Figure 17: Proportion of enclosed tessellation cells belonging to the individual clusters of the Medellin case study.

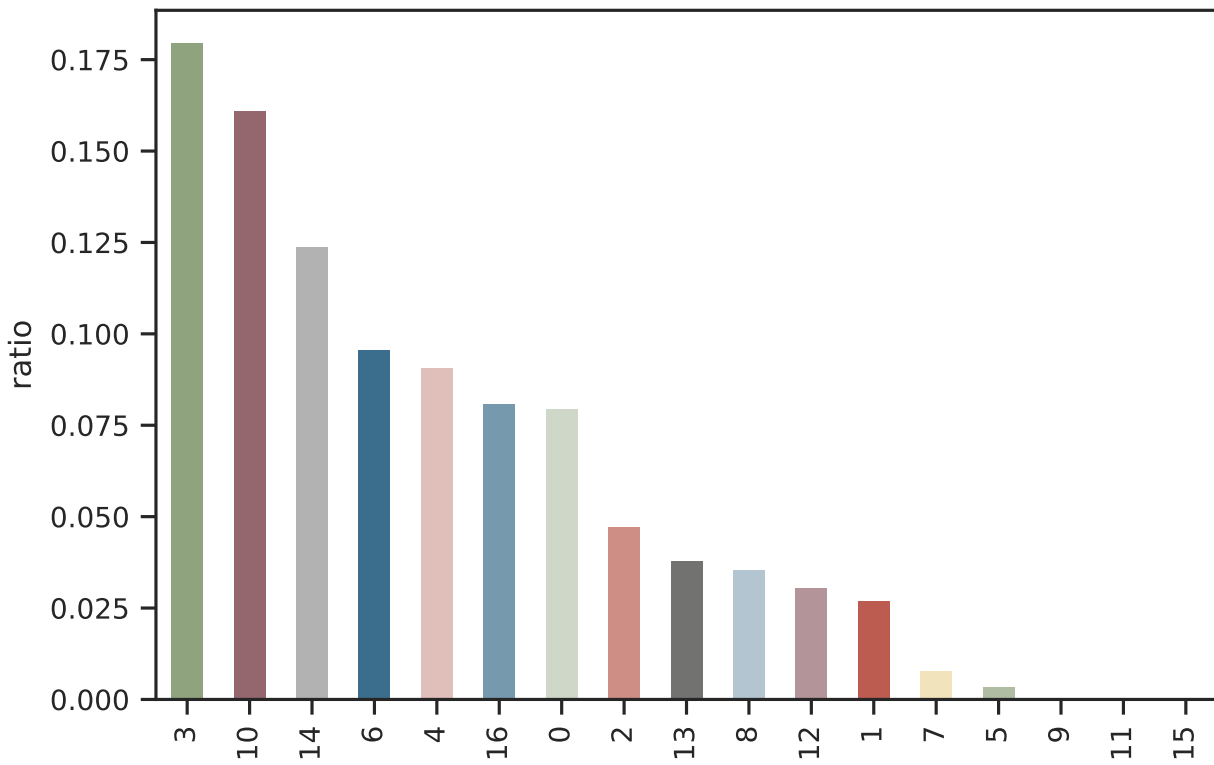


Figure 18: Proportion of enclosed tessellation cells belonging to the individual clusters of the Dar es Salaam case study.

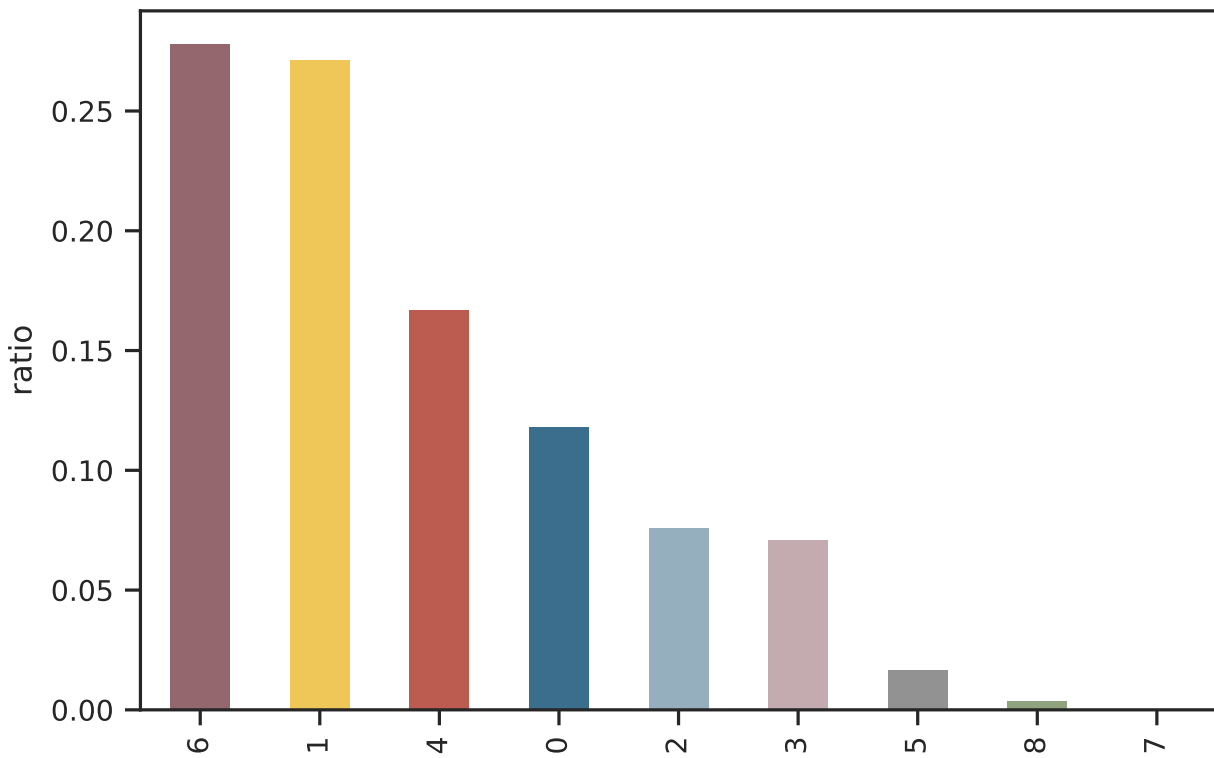


Figure 19: Proportion of enclosed tessellation cells belonging to the individual clusters of the Houston case study.

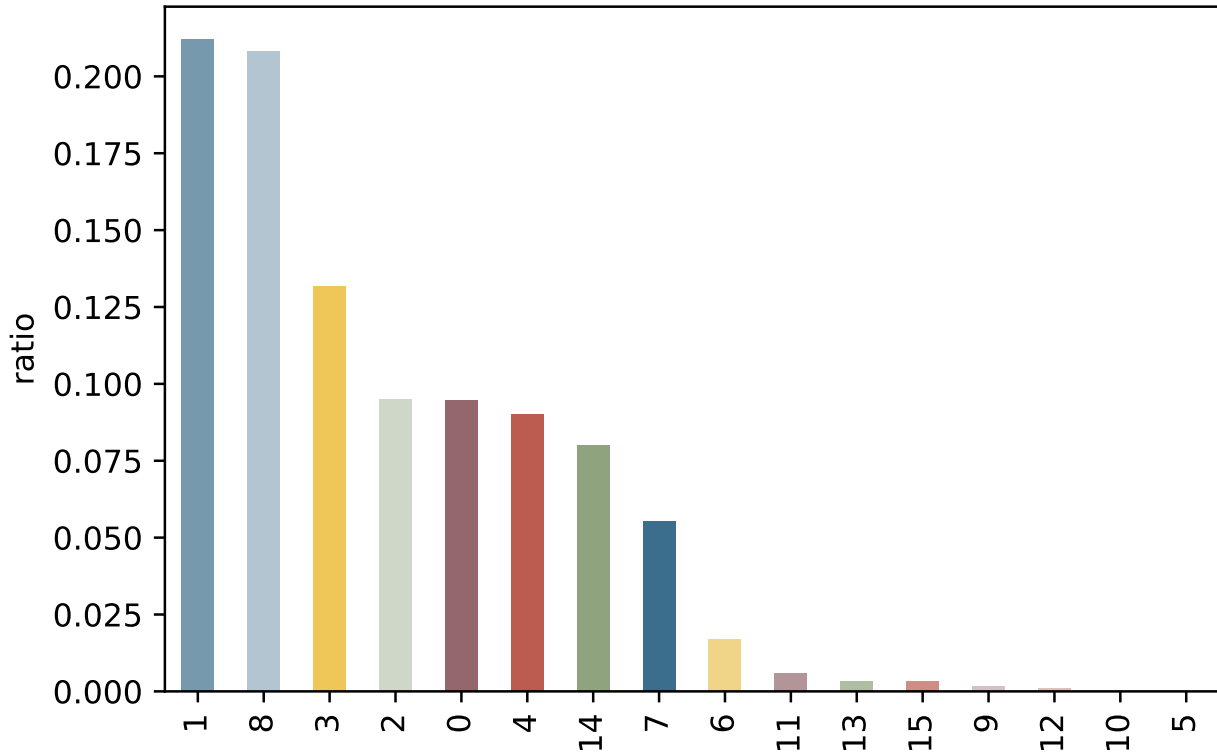


Figure 20: Proportion of enclosed tessellation cells belonging to the individual clusters of the Singapore case study.